INTERNATIONAL ATOMIC ENERGY AGENCY
UNITED NATIONS EDUCATIONAL, SCIENTIFIC AND CULTURAL ORGANIZATION
INTERNATIONAL CENTRE FOR THEORETICAL PHYSICS
I.C.T.P., P.O. BOX 586, 34100 TRIESTE, ITALY, CABLE CENTRATOM TRIESTE

UNITED NATIONS INDUSTRIAL DEVELOPMENT ORGANIZATION

INTERNATIONAL CENTRE FOR SCIENCE AND HIGH TECHNOLOGY

c/o INTERNATIONAL CENTRE FOR THEORETICAL PHYSICS 34100 TRIESTE (ITALY) VIA GRIGNANO, 9 (ADRIATICO PALACE) P.O. BOX 586 TELEPHONE (040) 224572 TELEFAX (040) 224575 TELEX 460449 SPH I

SMR/543 - 18

EXPERIMENTAL WORKSHOP ON
HIGH TEMPERATURE SUPERCONDUCTORS AND RELATED MATERIALS
(BASIC ACTIVITIES)

(11 February - 1 March 1991)

" Optical Properties of High T_c Superconductors "

presented by:

K. KAMARAS
Hungarian Academy of Sciences
Central Research Institute for Physics
P.O. Box 49
1525 Budapest
Hungary

OUTLINE

TALK 1

MEASUREMENT AND EVALUATION FUNDAMENTALS

LOW-T_c SYSTEMS

NORMAL-STATE OPTICAL PROPERTIES OF HIGH-T_c SYSTEMS

TALK 2

SUPERCONDUCTING STATE OF HTSC

E-PH COUPLING EFFECTS

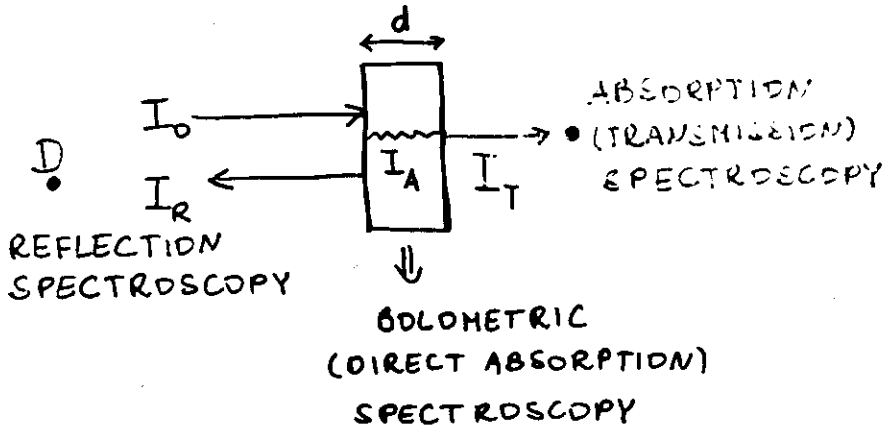

$$I_0 = I_R + I_A + I_T$$

$$I_R = R \cdot I_0$$

$$I_A = I_0(1-R)e^{-\alpha d}$$

$$R = \frac{(n-1)^2+k^2}{(n+1)^2+k^2}$$

$$\alpha = \frac{4\pi k}{\lambda}$$

$$\tilde{N} = n + ik = \sqrt{\tilde{\varepsilon}}$$

OPTICAL CONSTANTS

$\hat{\varepsilon} = \varepsilon_1 + i\varepsilon_2 \qquad \hat{n} = n + ik \qquad \hat{\sigma} = \sigma_1 + i\sigma_2$

$$\varepsilon_1 = n^2 - k^2 = 1 - \frac{4\pi\sigma_2}{\omega}$$

$$\varepsilon_2 = 2nk = \frac{4\pi\sigma_1}{\omega}$$

$$R = \frac{(n-1)^2 + k^2}{(n+1)^2 + k^2} = \left| \frac{1-\sqrt{\varepsilon}}{1+\sqrt{\varepsilon}} \right|^2$$

$R \rightarrow \varepsilon_1, \sigma_1$ via Kramers-Kronig analysis:

$$\Theta(\omega) = \frac{\omega}{\pi} P \int_0^\infty \frac{\ln R(\omega') - \ln R(\omega)}{\omega^2 - \omega'^2} d\omega'$$

$$\tilde{n} = n + ik = \left(\varepsilon_1 + i\frac{4\pi}{\omega}\sigma^{1/2}\right) = \frac{1+\sqrt{R}\,e^{i\theta}}{1-\sqrt{R}\,e^{i\theta}}$$

Reflectivity measurements:

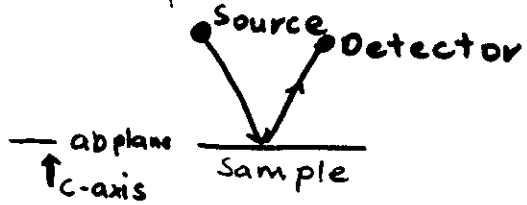

- home-made FIR spectrometer (McMaster) 40 - 1000 cm^{-1}
- BRUKER FTIR 100 - 3000 cm^{-1}
- PE grating spectrometer 1000 - 45000 cm^{-1}
- metal overcoating - normalize, correct for surface

Kramers-Kronig analysis of reflectance:

$$\Theta(\omega) = \frac{\omega}{\pi} P \int_0^\infty \frac{\ln R(\omega') - \ln R(\omega)}{\omega^2 - \omega'^2} d\omega'$$

Then

$$N = n + ik = \left(\varepsilon_1 + i\frac{4\pi}{\omega}\sigma_1\right)^{1/2} = \frac{1+\sqrt{R}\,e^{i\theta}}{1-\sqrt{R}\,e^{i\theta}}$$

Extrapolation procedure:

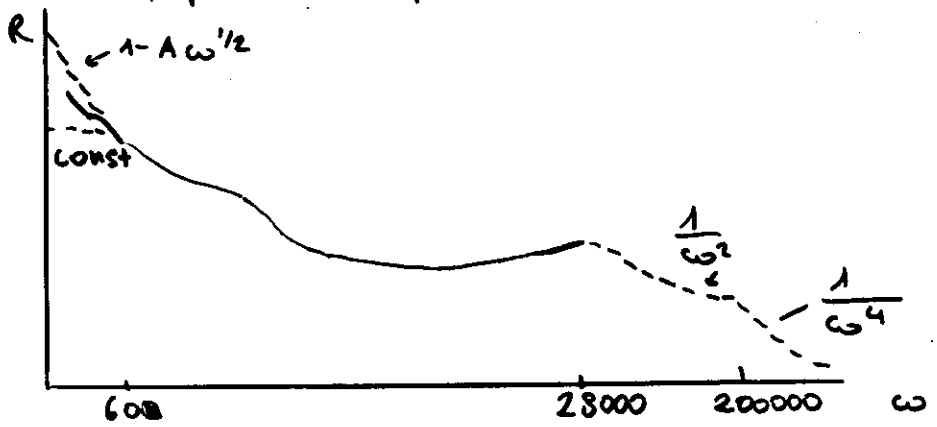

Infrared response of solids

a) Reflectance $R(\omega) = \left|\frac{\sqrt{\varepsilon} - 1}{\sqrt{\varepsilon} + 1}\right|^2$

b) $\varepsilon = \varepsilon_1 + i\varepsilon_2$ dielectric function

c) conductivity $\sigma(\omega) = \frac{\omega \varepsilon_2}{4\pi}$

Examples:

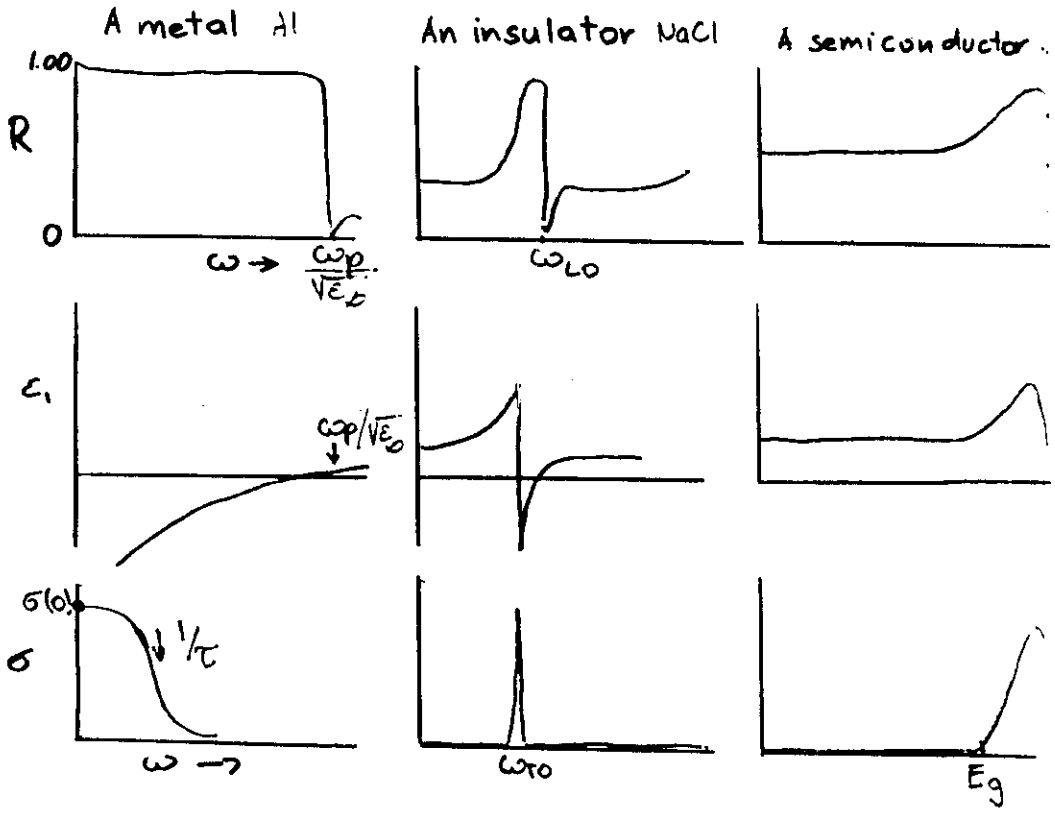

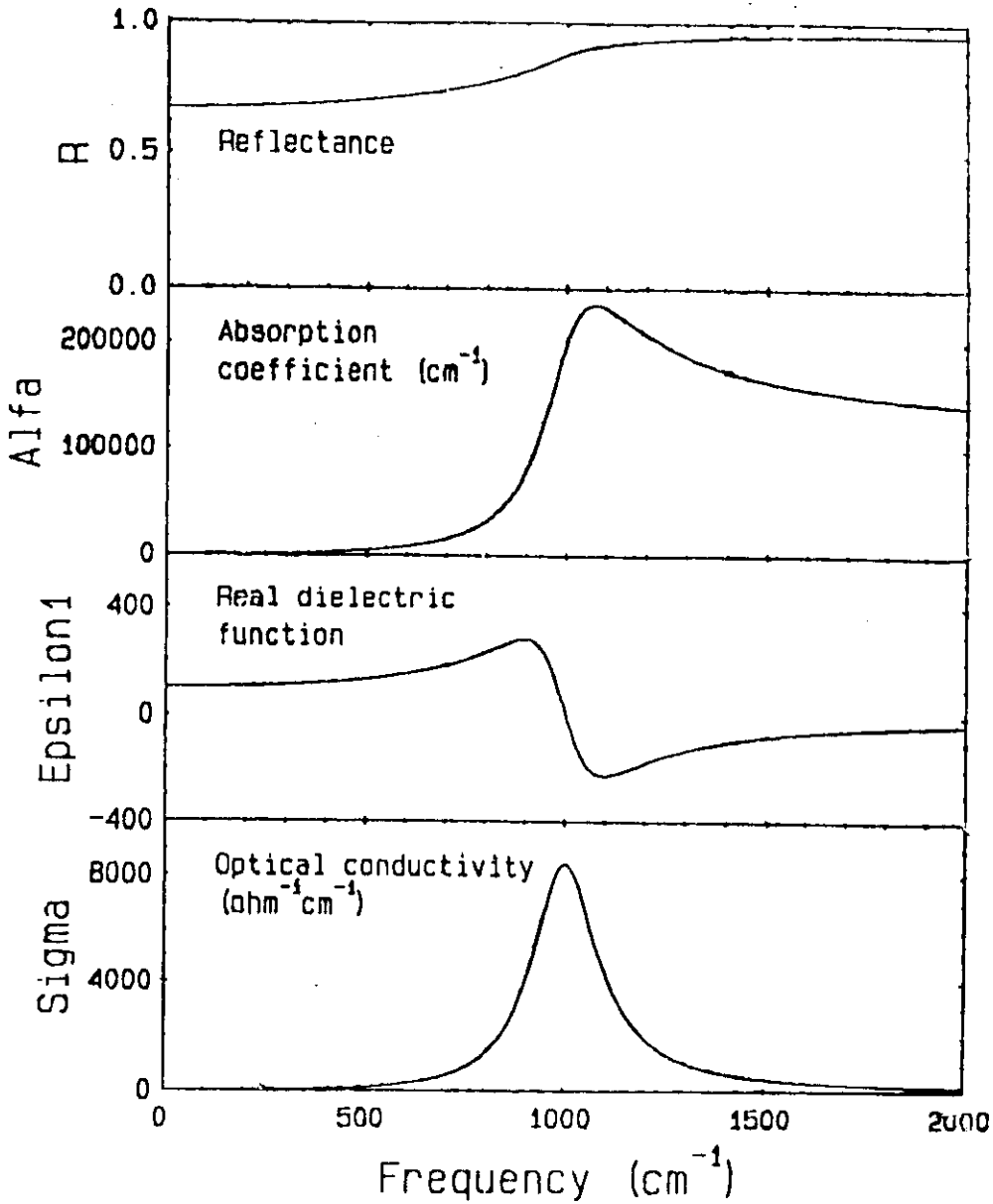

Drude conductivity:

$$4\pi\sigma(\omega) = \frac{\omega_p^2 \tau}{1+\omega^2\tau^2}$$

$$\omega_p^2 = \frac{4\pi N e^2}{m^*}$$

$$\tau = \frac{l}{v_F}$$

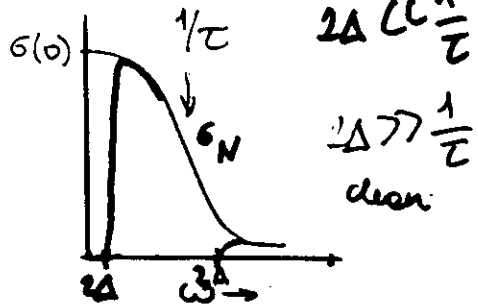

d.

$2\Delta \ll \frac{1}{\tau}$

$2\Delta \gg \frac{1}{\tau}$

clean

Temperature dependence:

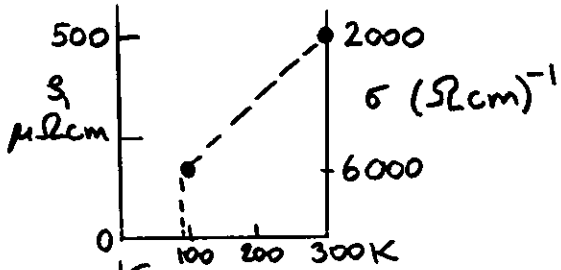

$$\int \sigma(\omega)\, d\omega = \frac{\omega_p^2}{8}$$

Conductivity sum rule

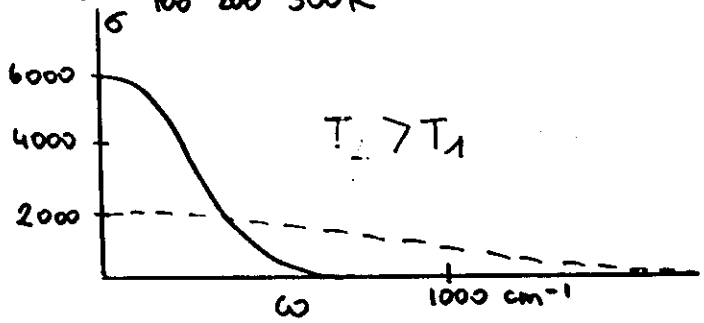

EXCITATIONS OF BOUND ELECTRONS

$$\varepsilon = \varepsilon_\infty + \sum_i \frac{4\pi n_i e^2}{m(\omega_i^2 - \omega^2 - i\gamma\omega)} =$$

$$= \varepsilon_\infty + \sum_i \frac{\omega_{pi}^2}{\omega_i^2 - \omega^2 - i\gamma\omega}$$

MOLECULAR EXCITATIONS (LOCALIZED)

CHARGE-TRANSFER EXCITATIONS

INTERBAND TRANSITIONS (DELOCALIZED)

Fitting Reflectances to a Model

a) Assume some form for the dielectric function:

$$\varepsilon(\omega) = \varepsilon_\infty + \frac{\omega_p^2}{(-\omega^2 - i\omega\Gamma)} + \sum_j \frac{\Omega_j^2}{(\omega_j^2 - \omega^2 - i\omega\gamma_j)}$$

Drude, free electron term — Classical oscillators

b) Calculate $R(\omega) = \left|\frac{\sqrt{\varepsilon} - 1}{\sqrt{\varepsilon} + 1}\right|^2$

c) Least squares fit $R(\omega)$ to experimenta data to find $\Omega_j, \omega_j, \gamma_j$ and $\varepsilon_\infty, \omega_p, \Gamma$

Region fitted $\leq$ region measured!

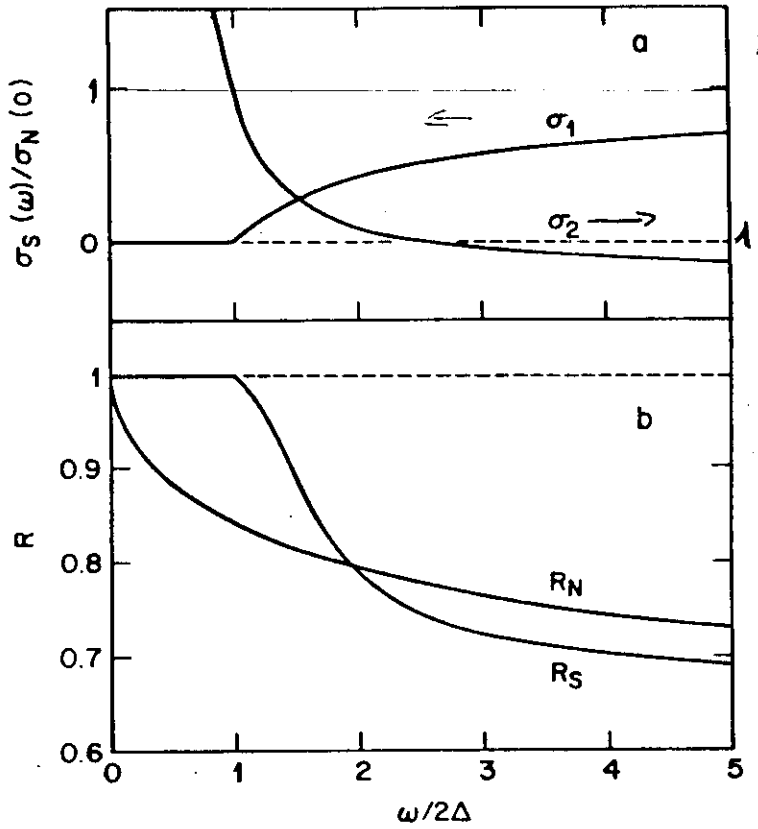

G.A. Thomas et al.: Phys. Rev. B 36, 846 (1987).

P.J. M. VAN BENTUM, P. WYDER

$A_s(4nm)/A_s(8nm) \approx C_0 + C_1\omega^2$. This quadratically increasing absorption was also reported in a number of experiments on small particles and on granular films [11, 12]. It seems reasonable to assume that the anomalous absorption of the superconducting film and the anomalous normal state absorption both have the same cause. An obvious approach to understand the physical process underlying the anomalous FIR behavior is to extract the complex conductivity from the experimental data using the inversion procedure described earlier in section 4. Using eqs. (13) and (14), we can determine the conductivity in a straightforward way. Above the gap, both absorption and transmission are largely determined by σ_1, therefore the inversion process is most accurate for σ_1. In fig. 14 we show the result of the inversion of the experimental data shown in figs. 11 and 12, using $R_s = 110\Omega$. The result for σ_1 in fig. 14(a) is in good agreement with the MB calculations (solid curve) for frequencies between Δ_0 and $4\Delta_0$. In fig. 14(b), σ_2 is considerably reduced compared with the MB calculations. above the gap the agreement is better, but these data are not very accurate due to the weak dependence of both absorption and transmission on σ_2. Fig. 14(b) suggests an ad hoc fit based on a renormalization of σ_2. A reasonable fit to the experimental σ_2 data was obtained with a reduced MB-curve given by $\sigma_2 = 0.7\sigma_2(MB)$ as shown with a dashed line in fig. 14(b). In fig. 15 we compare the experimental absorption and transmission of this film, with a theoretical calculation $\sigma_1 = \sigma_1(MB)$ and $\sigma_2 = \sigma_2(MB) \times 0.7$ and indeed find a good agreement. The reduction of σ_2 happens to be of the same magnitude as was calculated for the strong-coupling superconductor Pb by Nam [22]. It is therefore tempting to assume that the increase of T_c and Δ of ultrathin

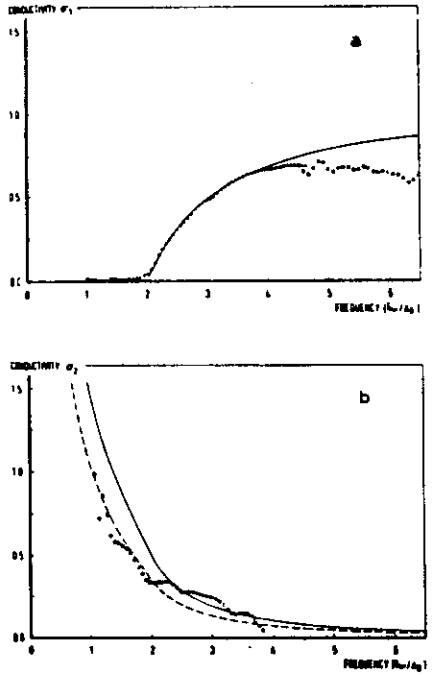

Fig. 14. a) (Δ) and (O): Experimental result for the real part of the conductivity σ_1 of film 6, using eq. (13) b) (O): Experimental result for the imaginary part of the conductivity σ_2 of film 6 according to eq. (14), using $R_s = 110\,\Omega$. The solid curves are calculated according to the weak-coupling theory. The dashed line in fig. 14(b) represents an ad hoc fit to the experimental points: $\sigma_2 = 0.7\sigma_2^{MB}$.

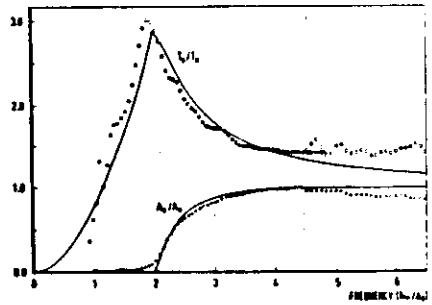

Fig. 15. Normalized absorption A_s/A_n (Δ) and transmission T_s/T_n (O) of film 6, together with a calculation using $R_n = 110\,\Omega$, $\sigma_1 = \sigma_1^{MB}$ and $\sigma_2 = 0.7\sigma_2^{MB}$.

HOLSTEIN EFFECT

(HOLSTEIN 1954; ALLEN 1971)

T. HOLSTEIN: PRB 96, 539 (1954)

P.B ALLEN: PRB 3, 305 (1971)

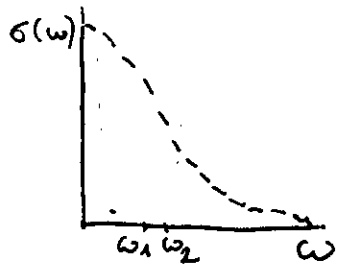

LOW T ($T \ll T_{DEBYE}$)

HIGH T ($k_B T > \hbar\langle\omega_{ph}\rangle$)

$\Gamma = (2\pi\lambda/\hbar)(kT + \hbar\langle\omega_{ph}\rangle/2)$

EXTENDABLE TO OTHER EXCITATIONS

(NOT NECESSARILY DIPOLE ACTIVE)

SUPERCONDUCTING STATE:

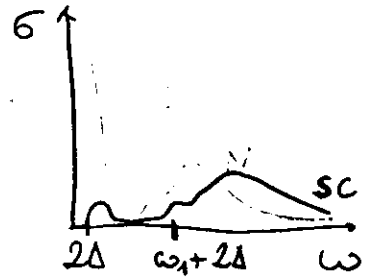

BY ANALOGY WITH LOW T_c SYSTEMS:

NORMAL STATE $\omega_p \Rightarrow n/m^*$

$\tau \Rightarrow \ell$

SC STATE $R \Rightarrow 2\Delta$

POSSIBLE HOLSTEIN EFFECT

$\downarrow$

$2\Delta, \lambda$

IN REALITY:

LOTS OF PROBLEMS!

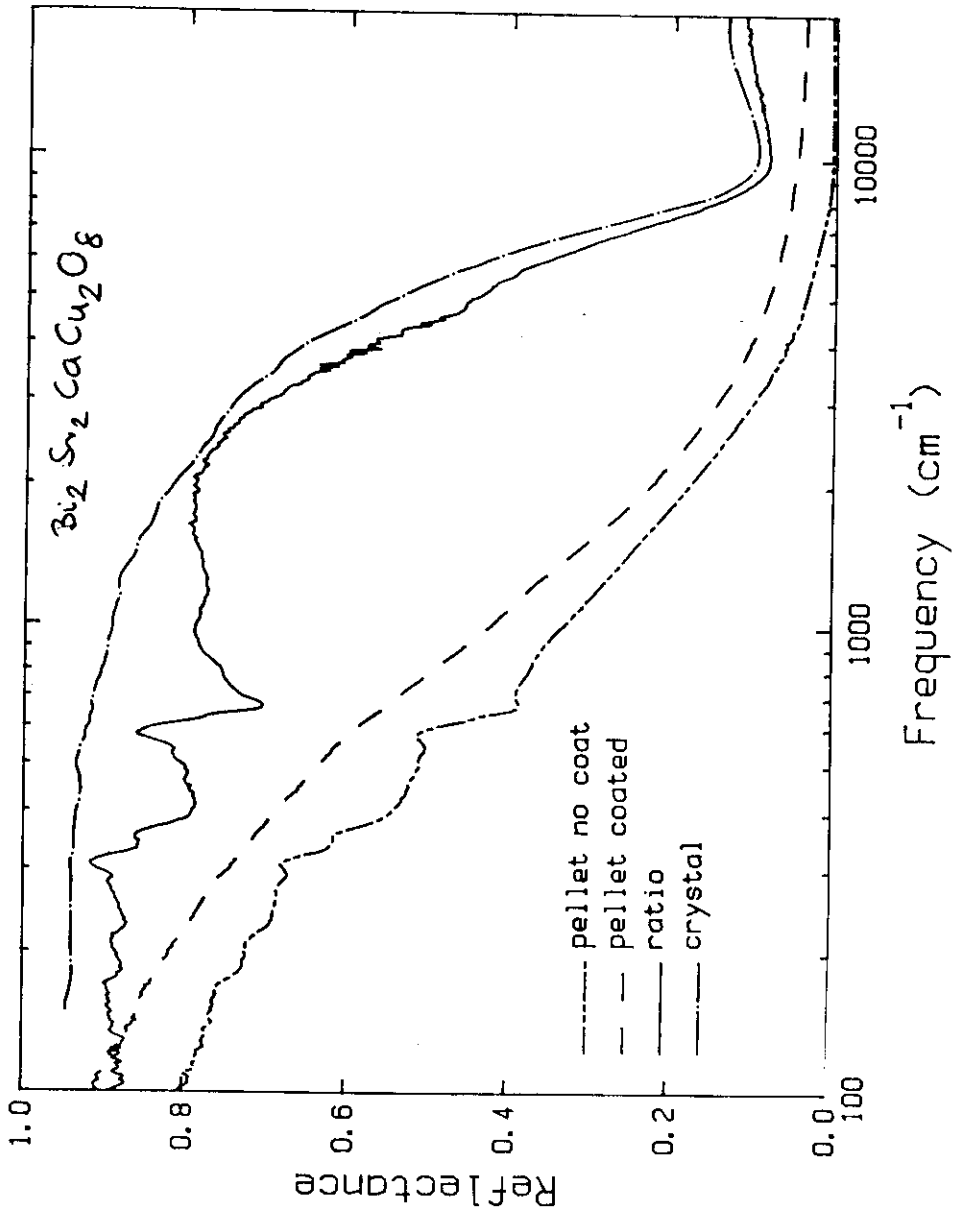

$T_c \sim 90°K$

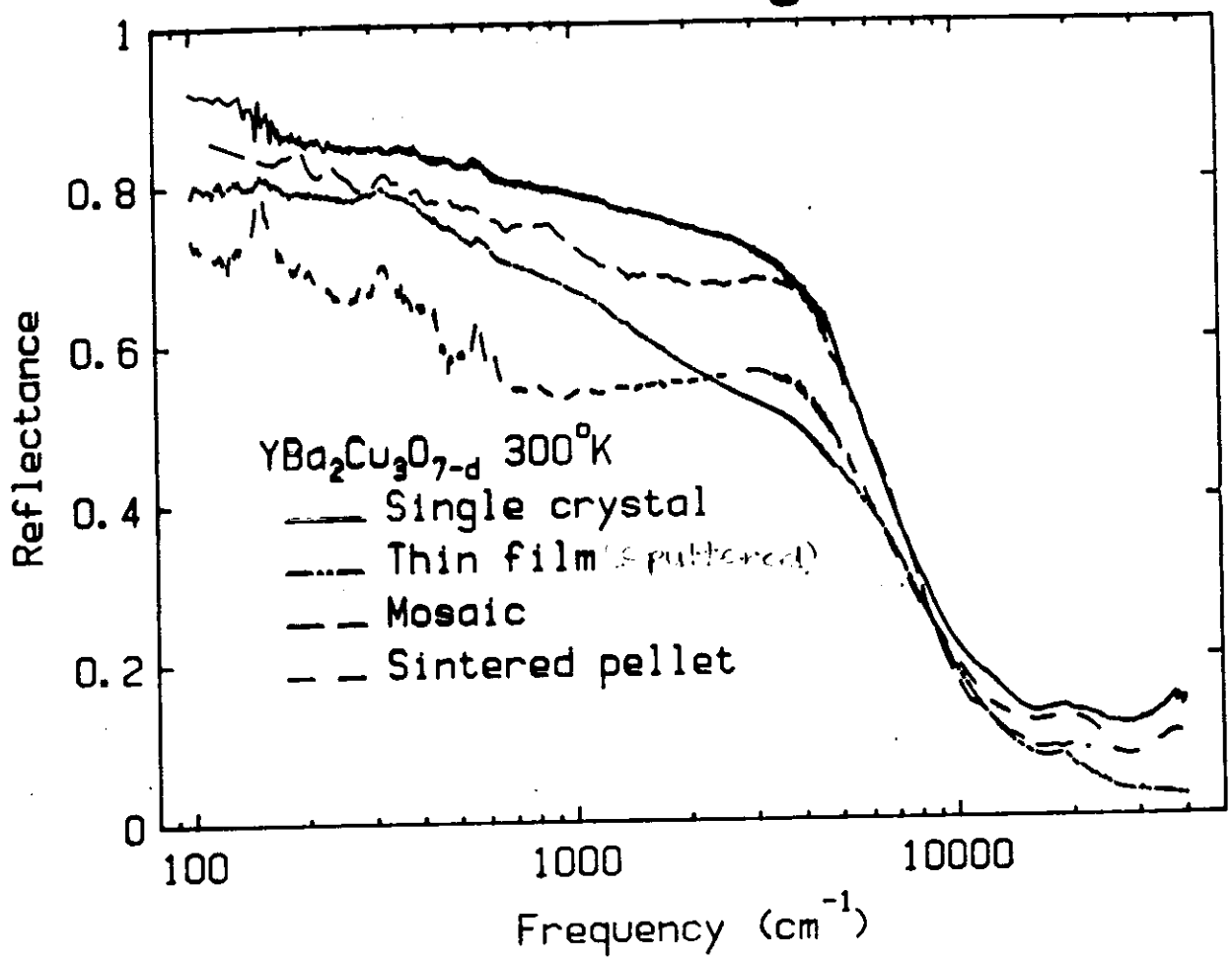
Reflectance
1
0.8
0.6
0.4
0.2
0
100
1000
10000
Frequency (cm^{-1})
$YBa_2Cu_3O_{7-d}$ 300°K
Single crystal
Thin film (sputtered)
Mosaic
Sintered pellet

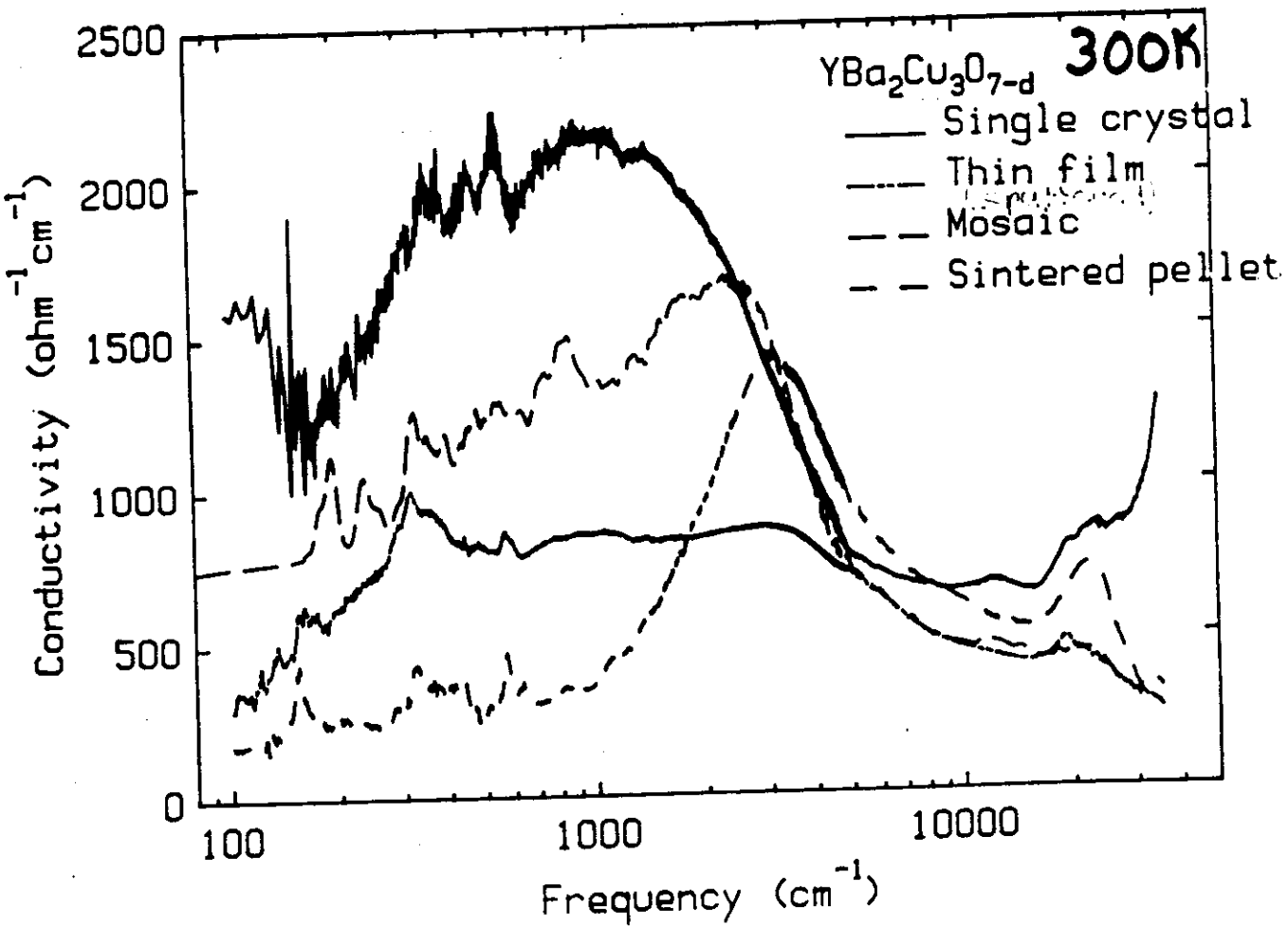
Conductivity (ohm^{-1}cm^{-1})
2500
2000
1500
1000
500
0
100
1000
10000
Frequency (cm^{-1})
$YBa_2Cu_3O_{7-d}$ 300K
Single crystal
Thin film (sputtered)
Mosaic
Sintered pellet

Z. Schlesinger et al: PRL 59, 1958 (1987)

$YBa_2Cu_3O_7$ crystal $\omega_p \cong 3eV$

$\tau \cong 10^{-15}$ s

$\parallel c$

$\ell = 1-3$ Å

$(v_F = 2 \cdot 10^7 \frac{cm}{s})$

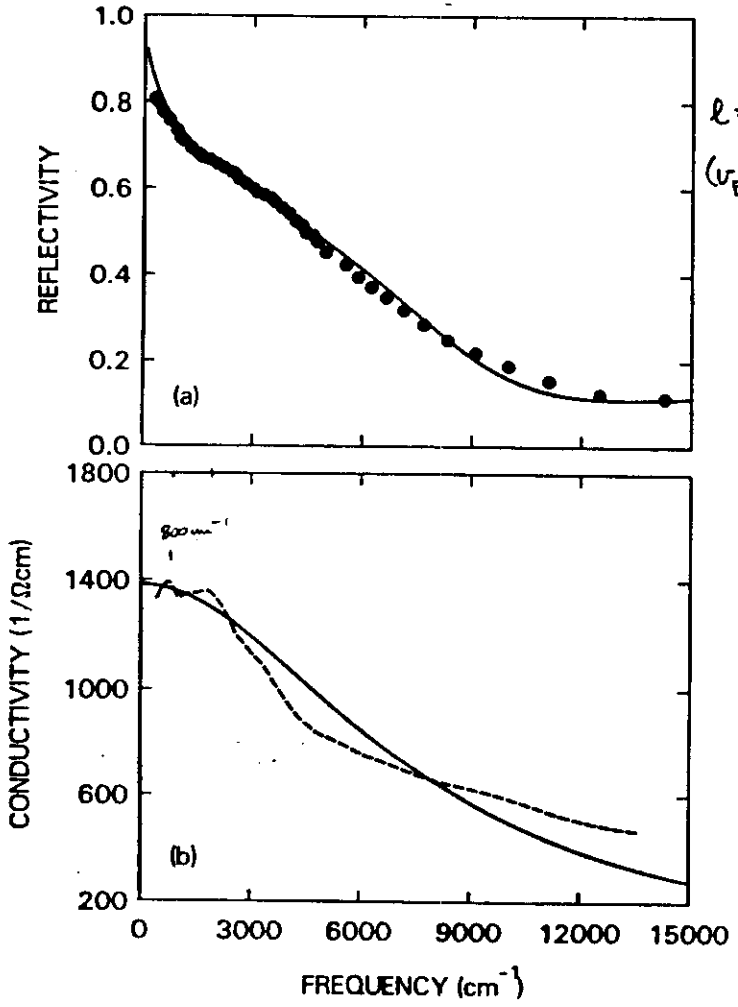

Simulation of Drude reflectivity
of $YBa_2O_{3.06}$ is a metal
$\sigma(T)$ is linear down to 100K

$\omega_p \cong 25000\,cm^{-1}$

$\omega_0 \cong 4$

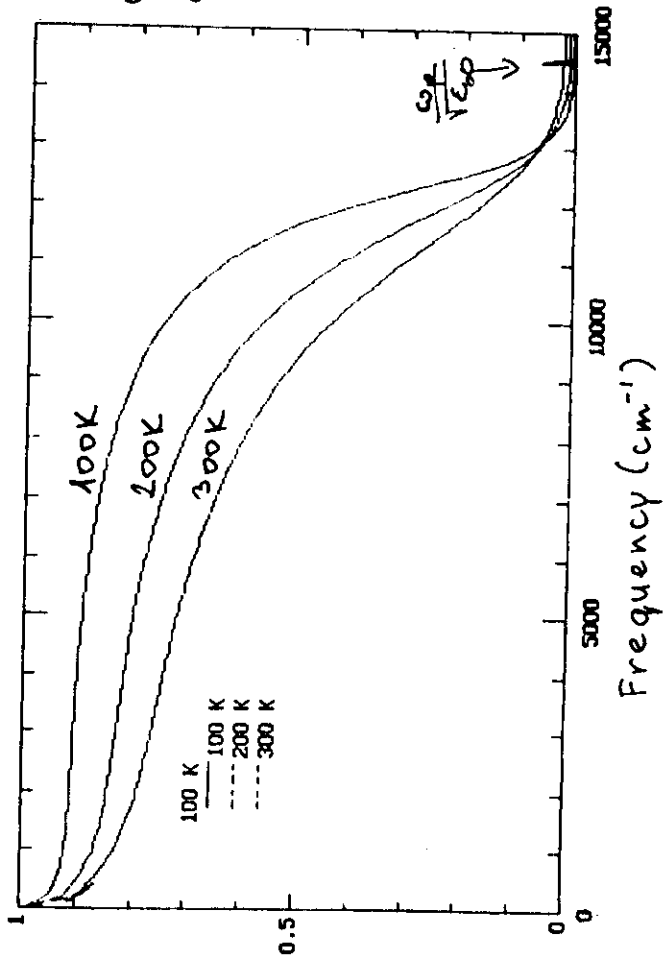

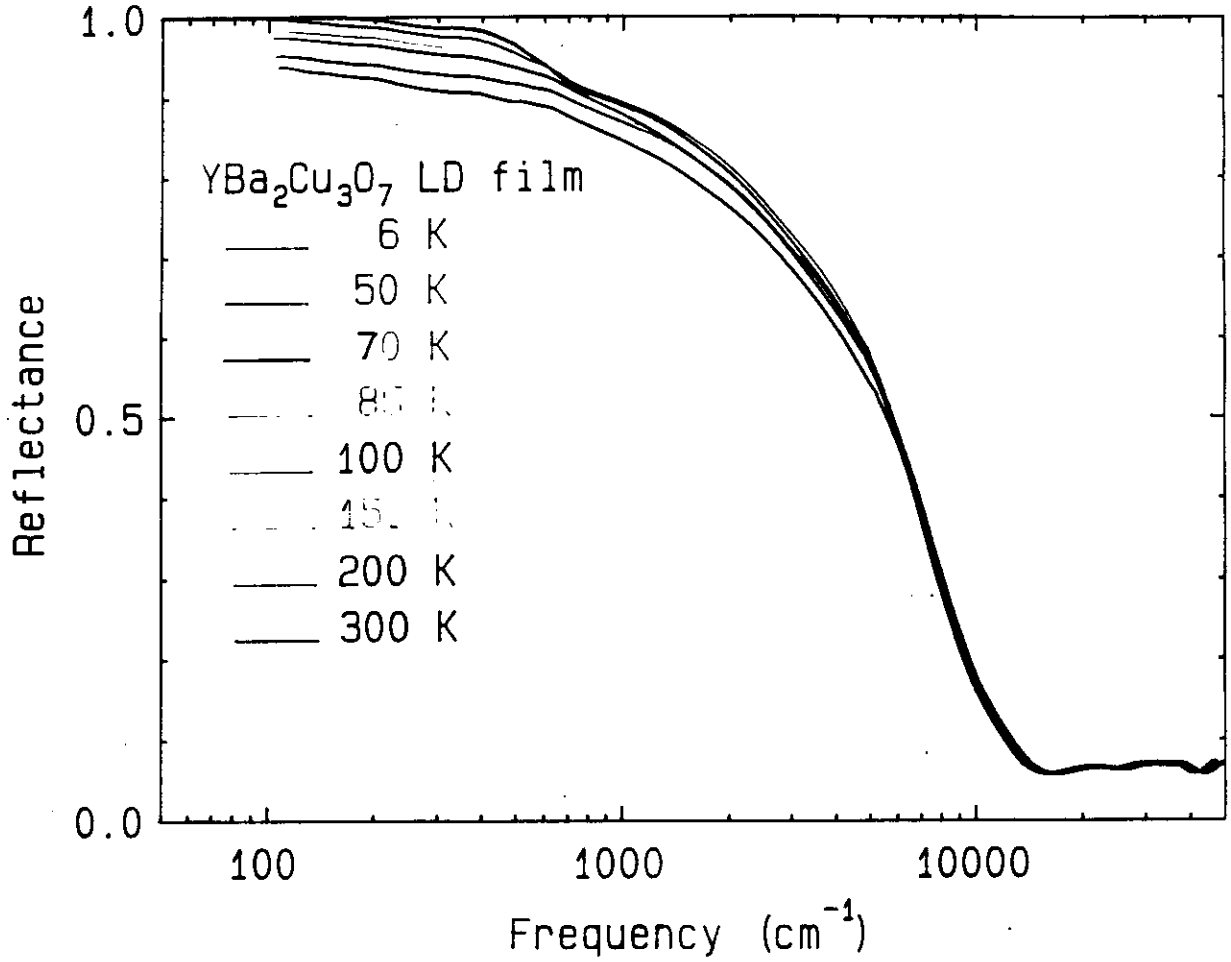

KAMARAS ET AL: PRL 64, 84 (1990)

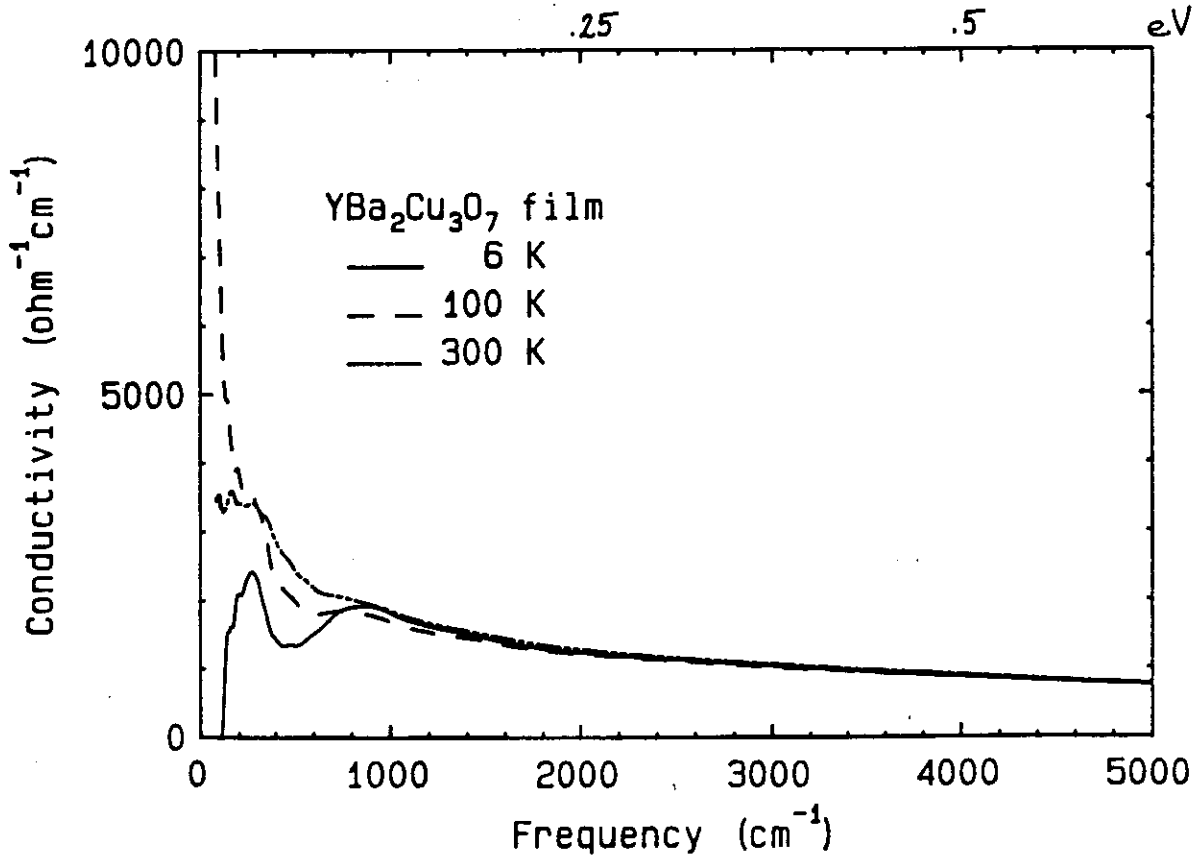

TIMUSK ET AL.: PRB 38, 6683 (1988)

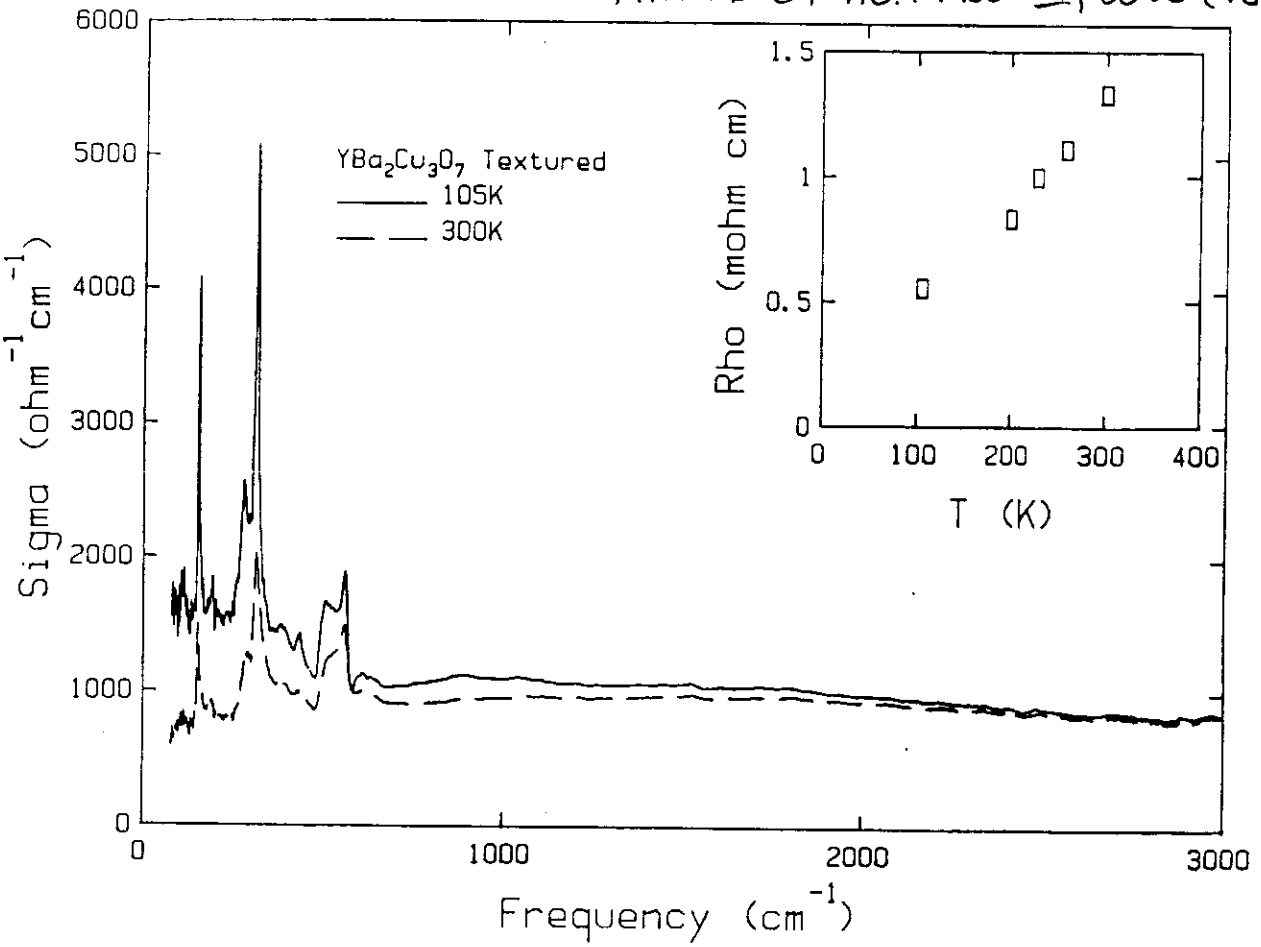

NORMAL STATE DIELECTRIC FUNCTION:

$$\varepsilon(\omega) = -\frac{\omega_{pD}^2}{\omega^2 + i\omega/\tau_D} + \frac{\omega_{MIR}^2}{\omega_{0,MIR}^2 - \omega^2 - i\omega\Gamma_{MIR}} + \sum_j \frac{S_j \omega_j^2}{\omega_j^2 - \omega^2 - i\gamma_j\omega} + \varepsilon_\infty$$

↓ FAR IR DRUDE PART

↓ MID-IR BAND

↓ PHONONS

↓ ~4

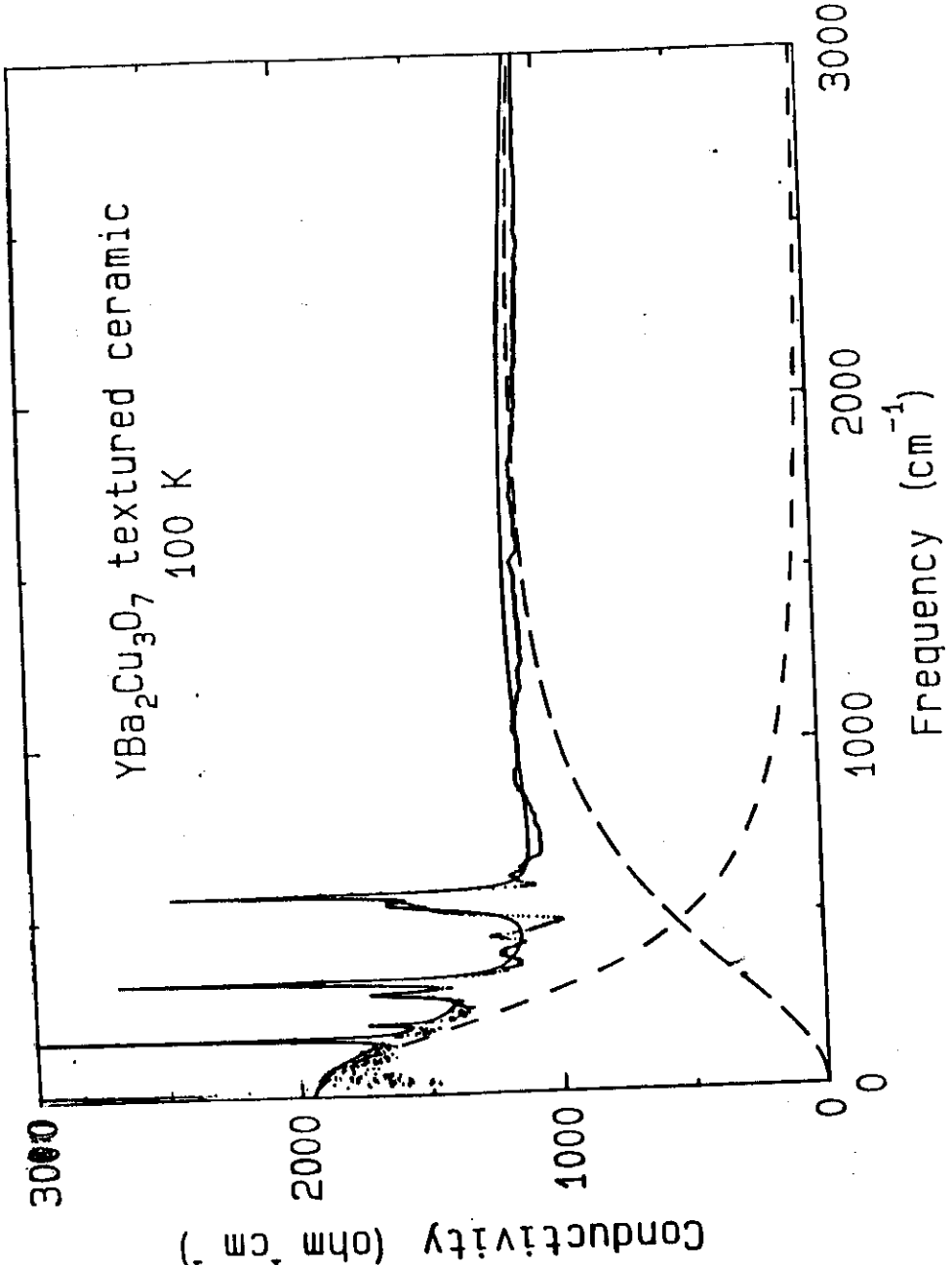

$YBa_2Cu_3O_7$ SPUTTERED FILM

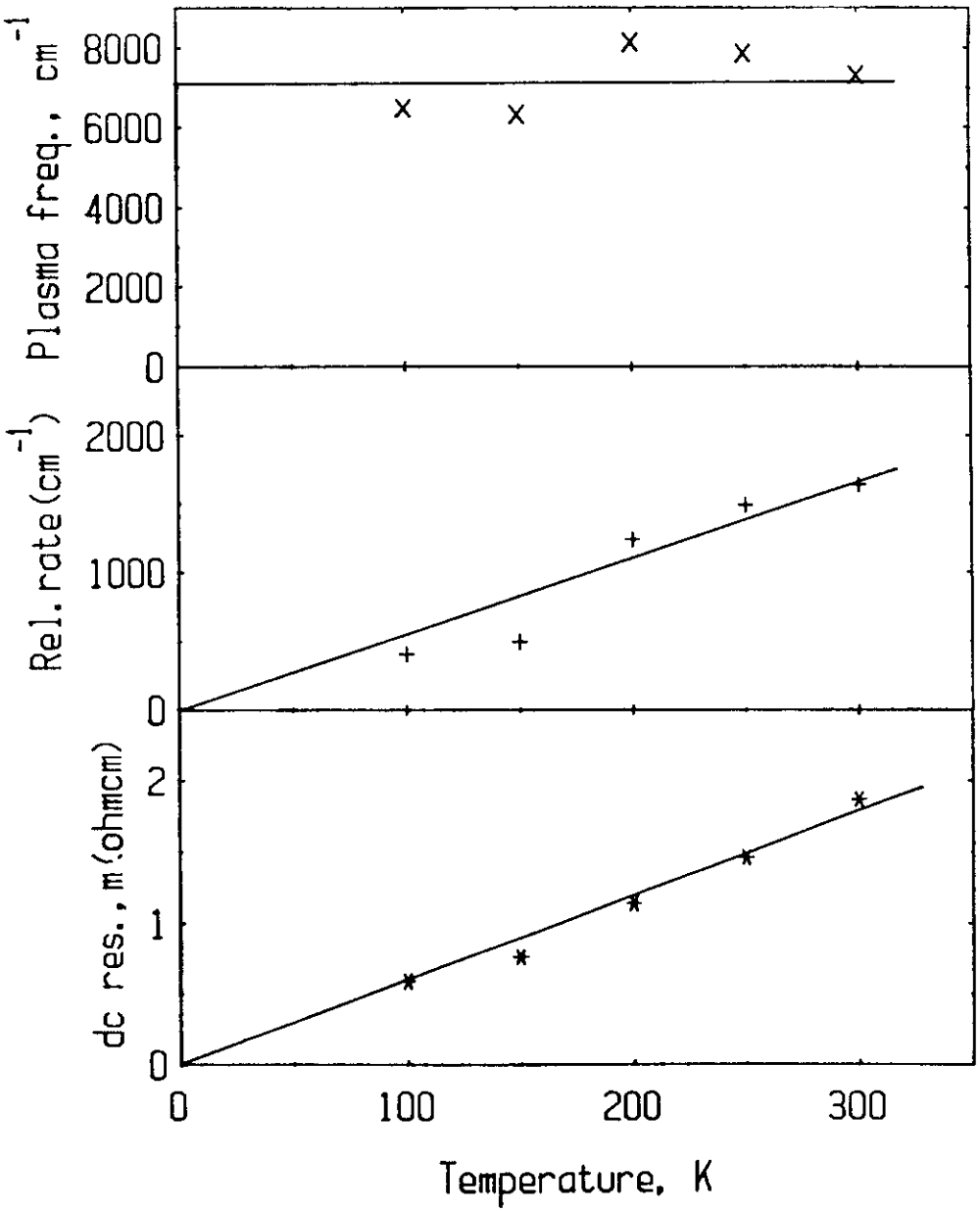

J. ORENSTEIN
1990
$YBa_2Cu_3O_{6+x}$

PRB 42, 6342
(1990)

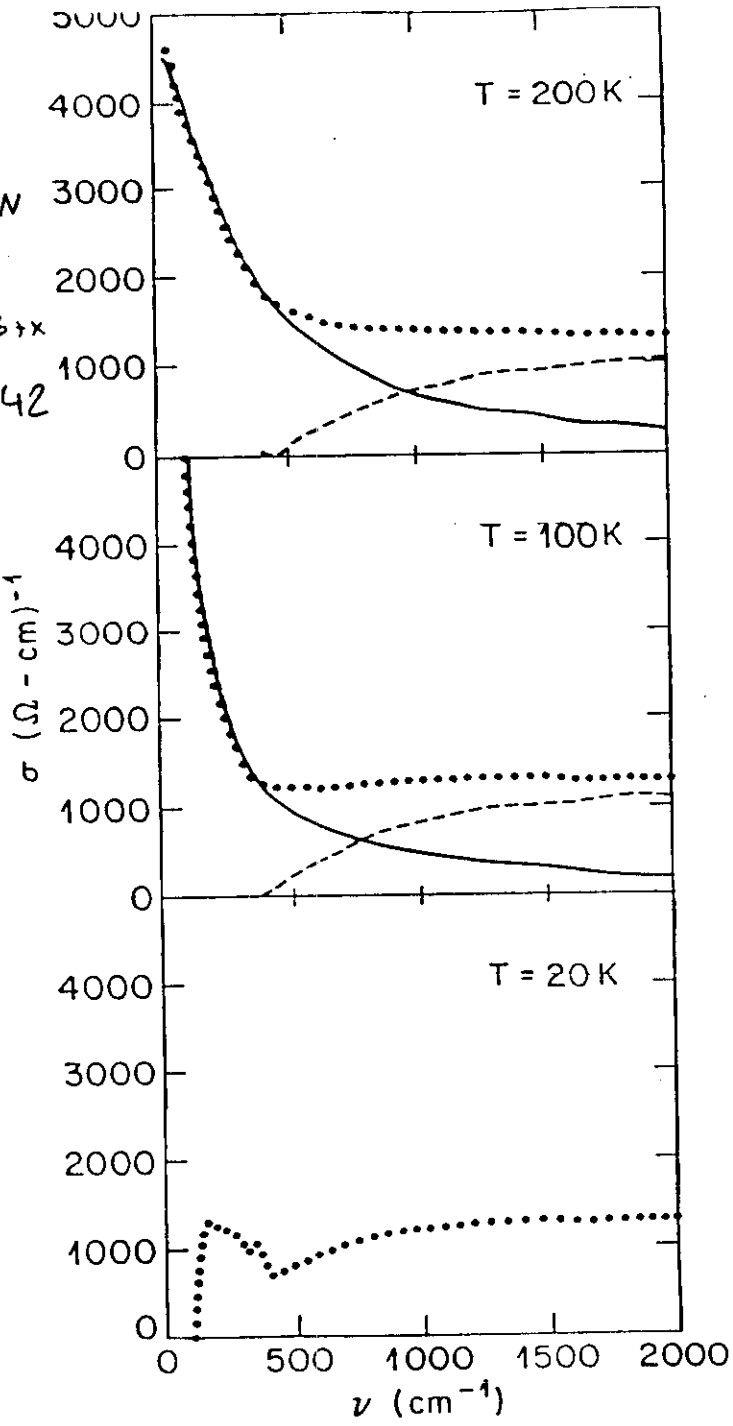

TEMPERATURE INDEPENDENT
MID-INFRARED ABSORPTION

DIRECT (IR ACTIVE)
CHARGE TRANSFER
VALENCE FLUCTUATIONS
ETC.

CT EXCITATIONS
ON CHARGE
RESERVOIR

INDIRECT
(IR INACTIVE, COUPLED)

PHONONS (HOLSTEIN)
MAGNONS (ORENSTEIN)
CHARGE + SPIN (VARMA)

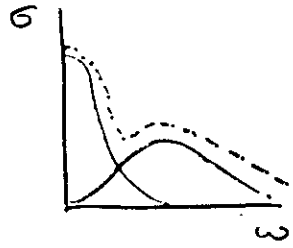

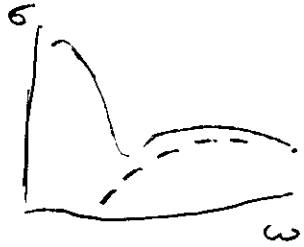

CONVENTIONAL SUPERCONDUCTORS:

$R = 1.00 \quad \omega < \omega_g$

"EARLY HIGH T_c" : $R < 1$ AT ANY ω

CIRCUMVENTING PROCEDURES:

- SCALE UP REFLECTIVITY

- PLOT R_S/R_N
  SHOULD HAVE MAXIMUM AT DOWNTURN OF R_S

- MORE ELABORATE METHODS TO TAKE INTO ACCOUNT:
  - PRESENCE OF "NORMAL" PHASE
  - C-AXIS ORIENTATION
  ETC.
  (MOSTLY EMA)

QUESTION: $R<1$ MATERIAL PROBLEM

OR INTRINSIC PROPERTY?

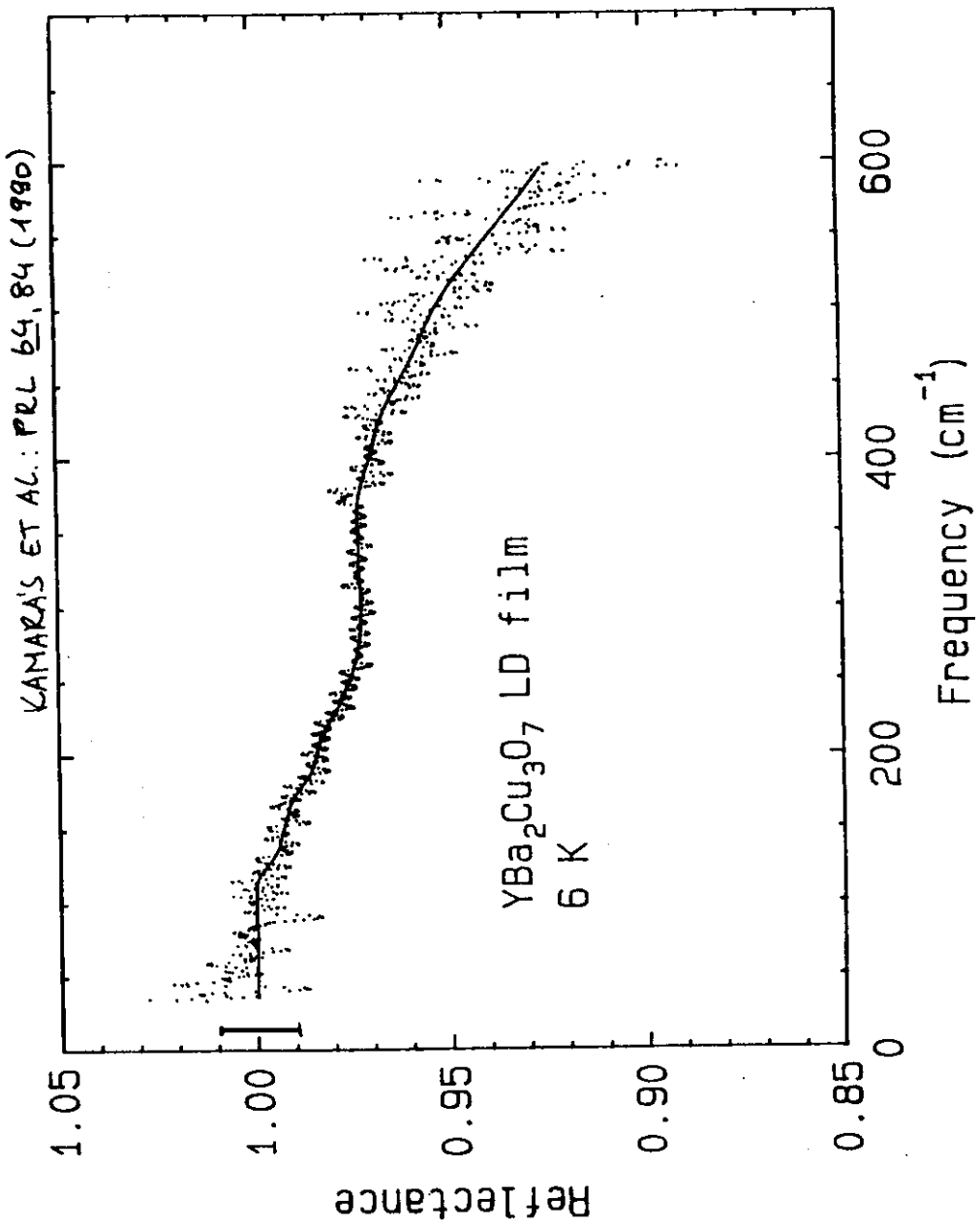

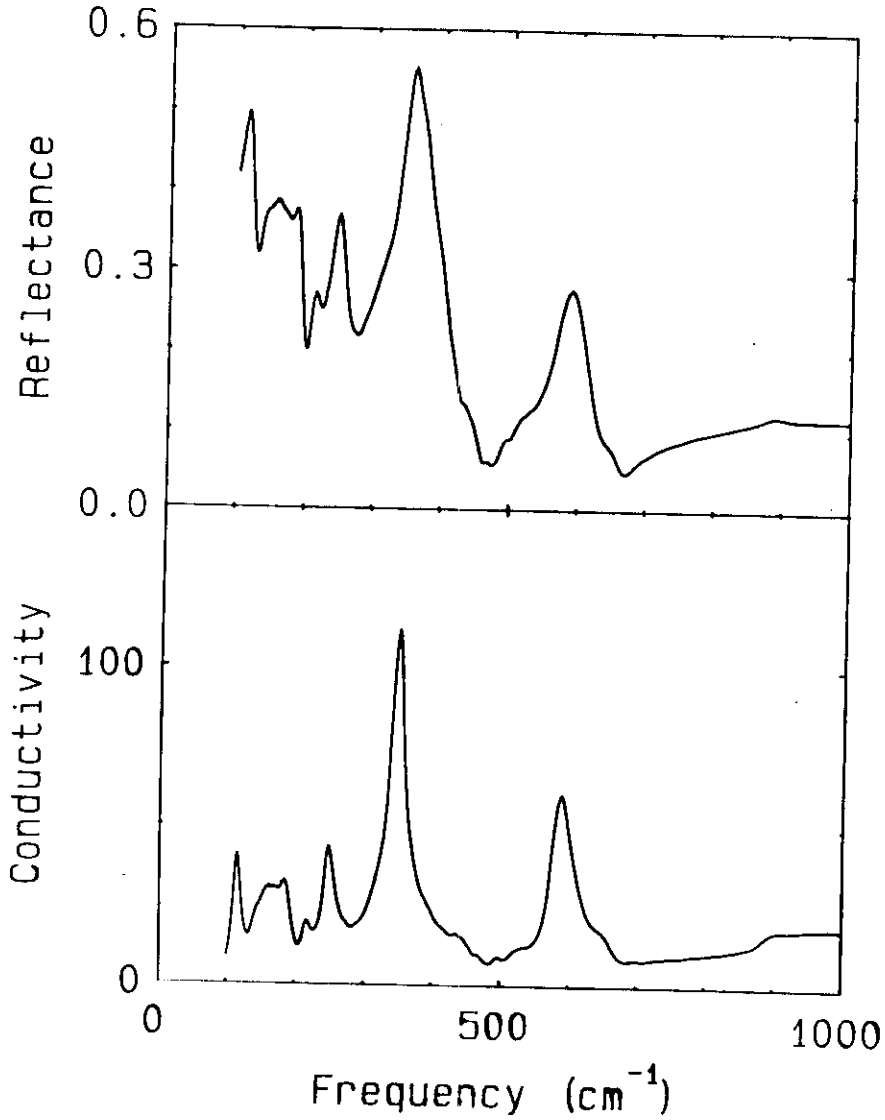
0.6
0.3
0.0
Reflectance
100
0
Conductivity
0
500
1000
Frequency (cm^{-1})

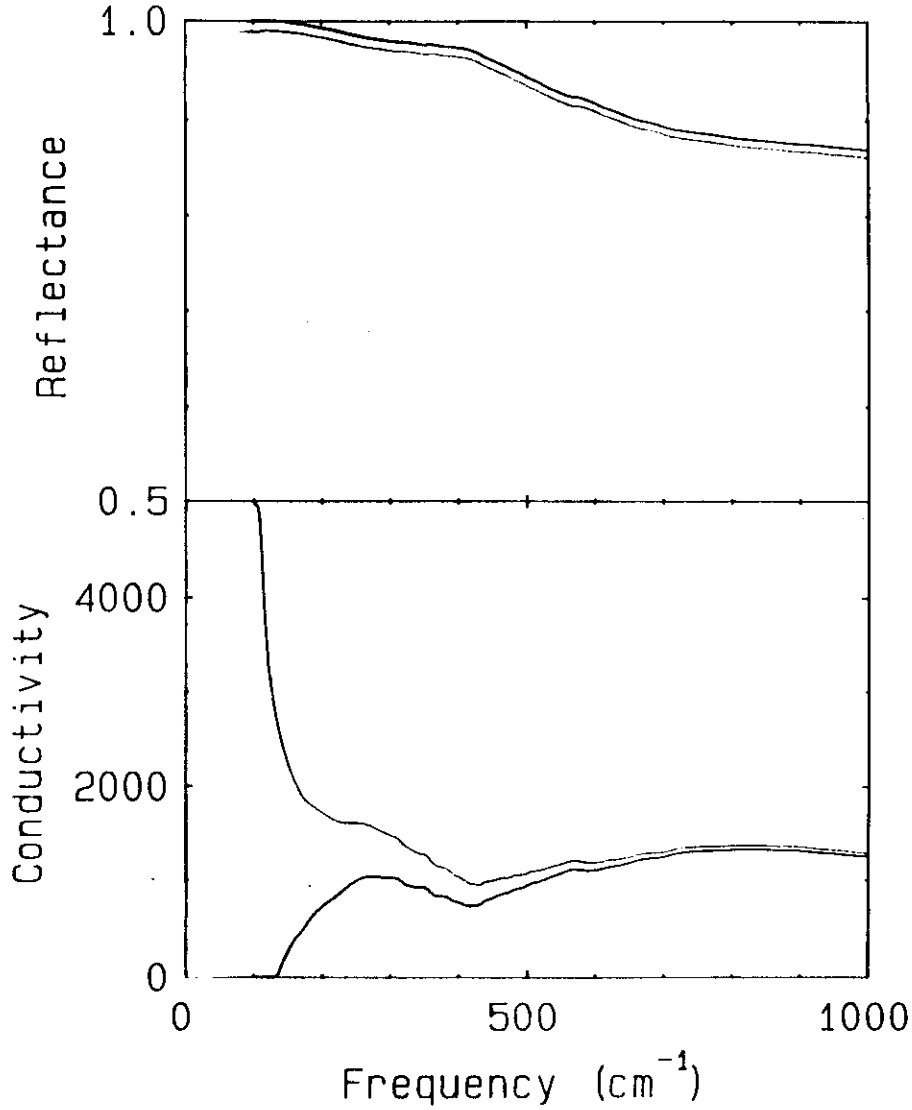
1.0
Reflectance
0.5
4000
2000
0
Conductivity
0
500
1000
Frequency (cm^{-1})

G.L. CARR ET AL. (1989)

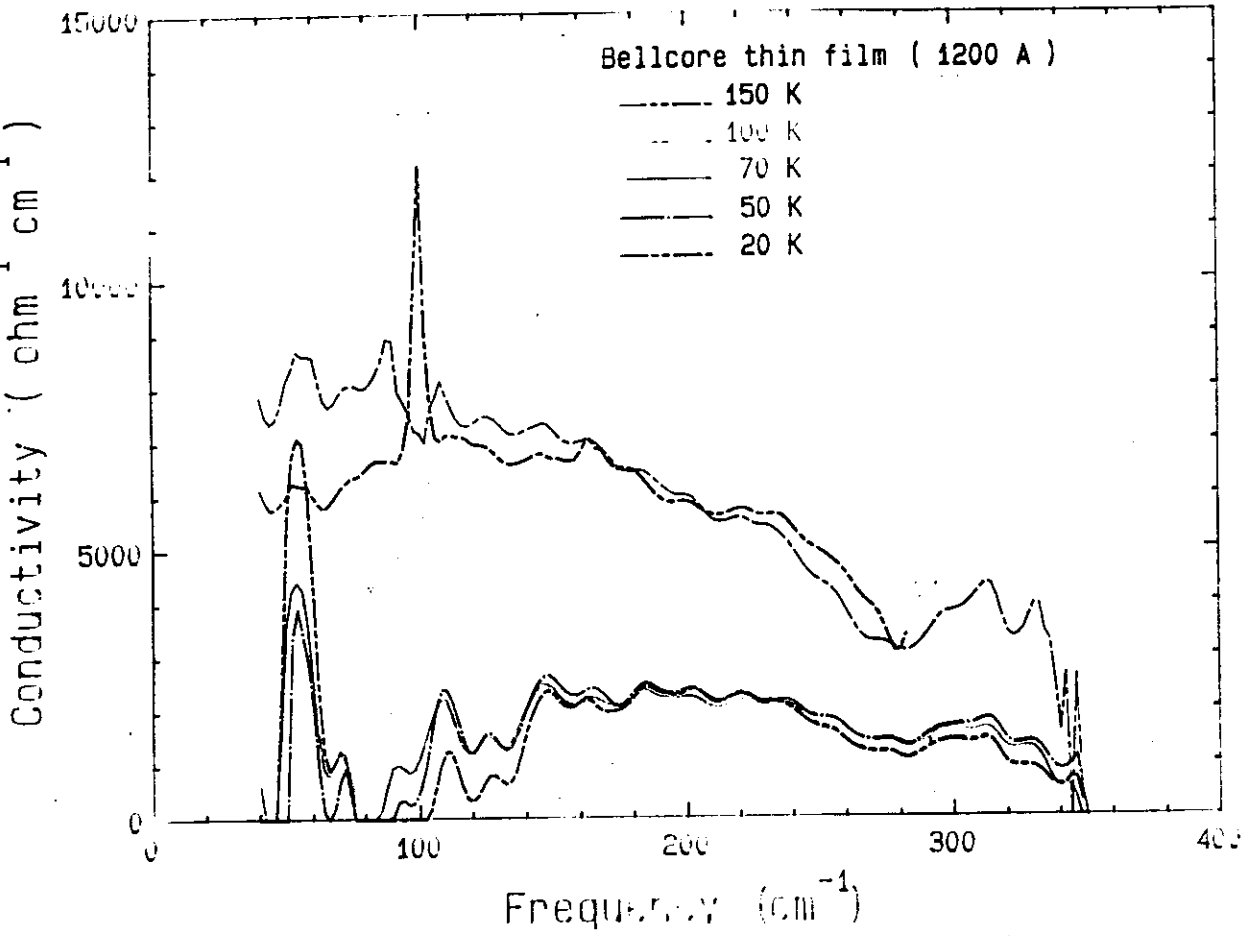

M. REEDYK ET AL.: PRB 38, 11981 (1988)

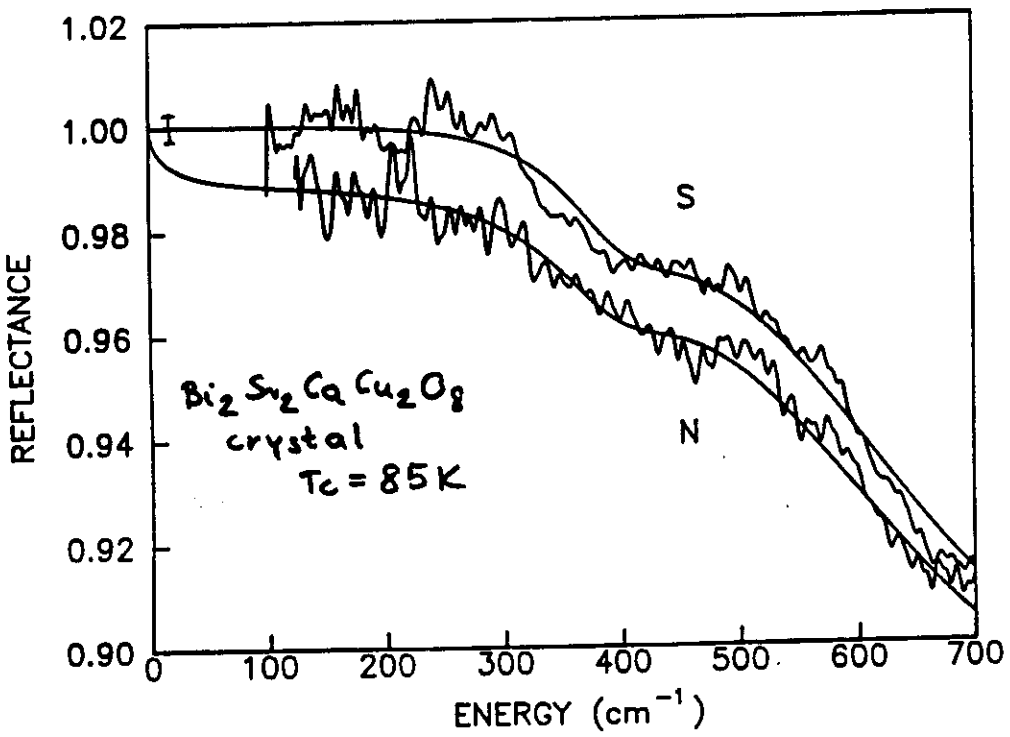

Fig. 3

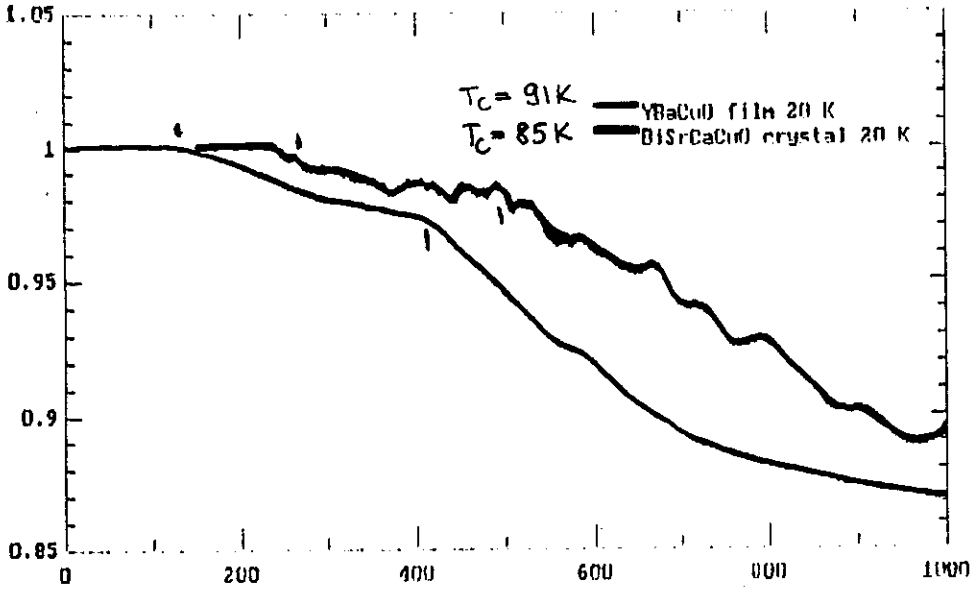
1.05
1
0.95
0.9
0.85
0
200
400
600
800
1000
T_c= 91K
T_c= 85K
YBaCuO film 20 K
BiSrCaCuO crystal 20 K
Frequency (cm-1)

5

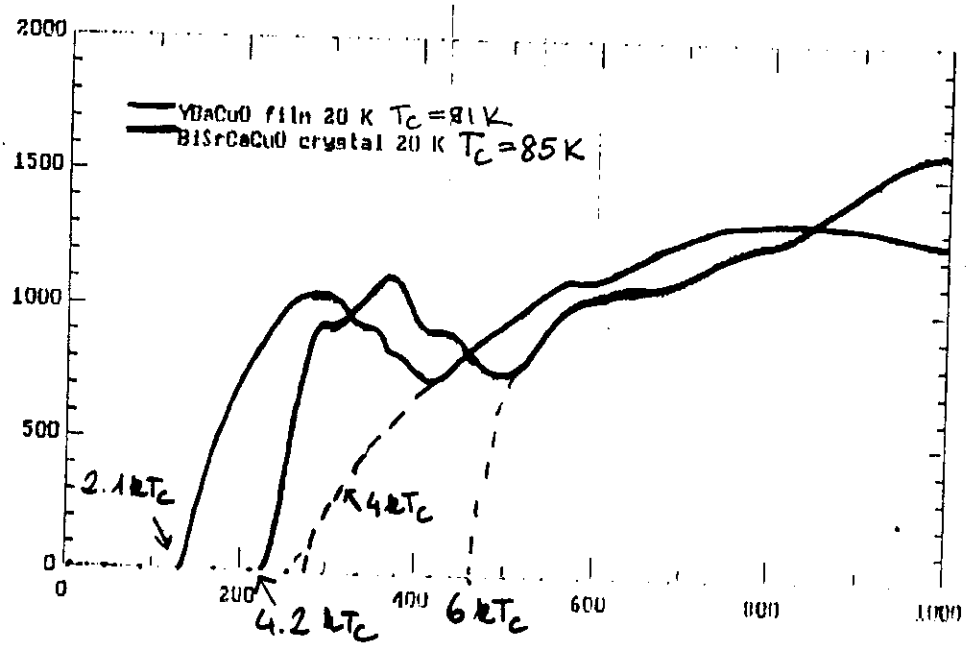
2000
1500
1000
500
0
0
200
400
600
800
1000
YBaCuO film 20 K T_c=91K
BiSrCaCuO crystal 20 K T_c=85K
2.1 kT$_c$
4 kT$_c$
4.2 kT$_c$
6 kT$_c$
Frequency (cm-1)

6

J. ORENSTEIN (1989)

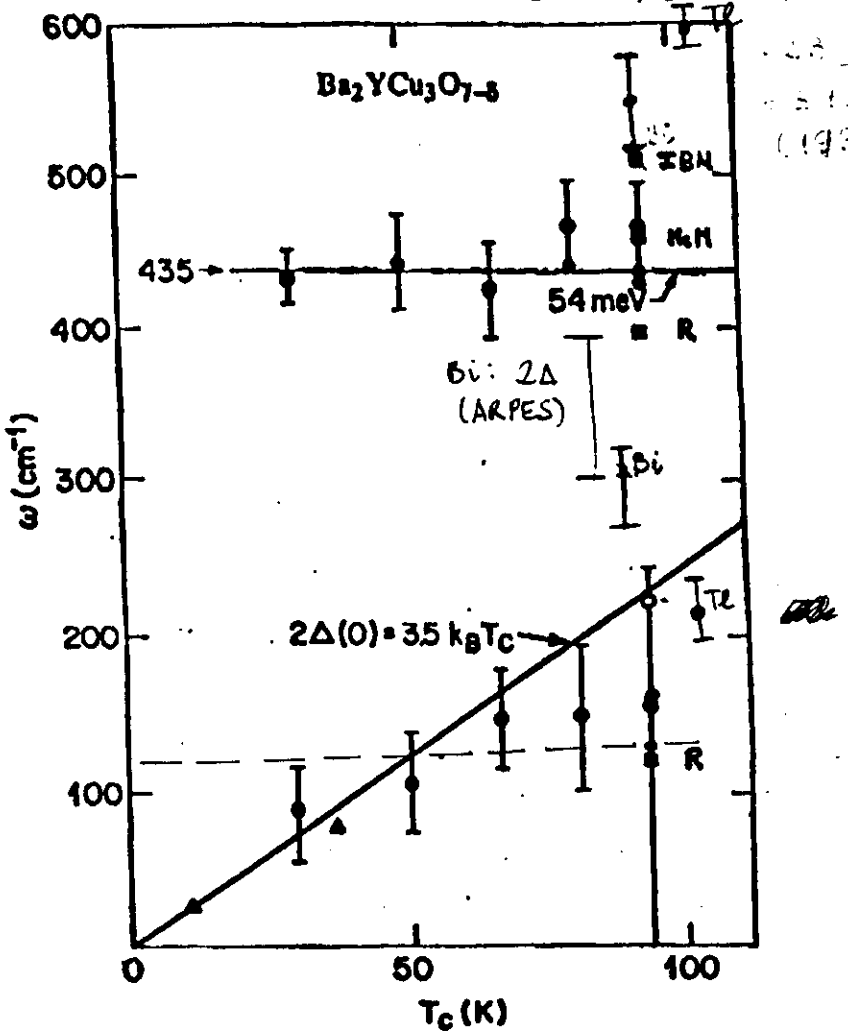

D.B. ROMERO ET AL. (1990)

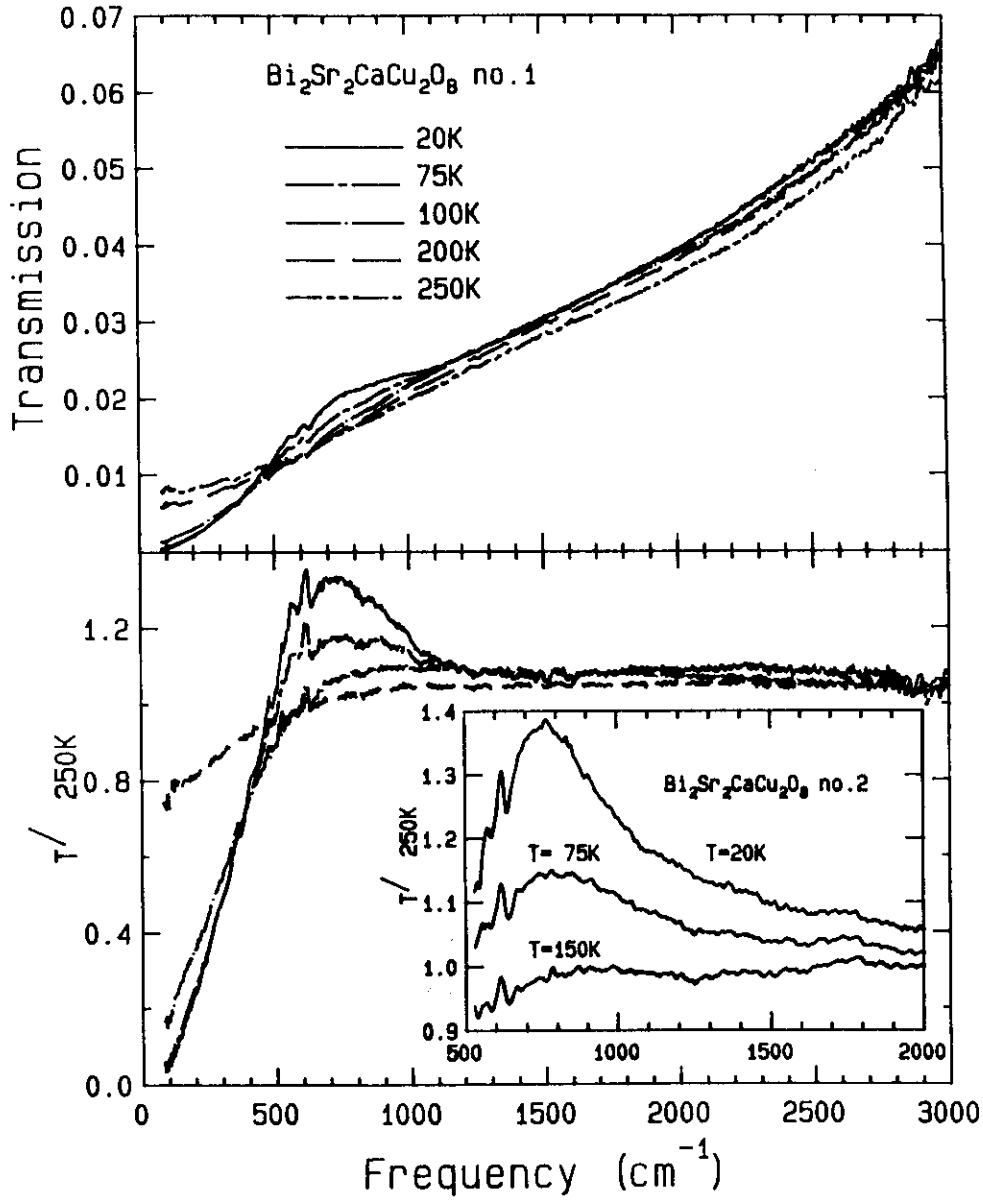

Fig 3

"GAP-LIKE FEATURES"
IN $Bi_2Sr_2CaCu_2O_8$

	2Δ
REFLECTIVITY:	
FIRST DOWNTURN	$4kT_c$
SECOND " "	$6kT_c$ NAIVE
	$3kT_c$ "MFL"
PHOTOEMISSION	$3-5kT_c$
TRANSMISSION	$12kT_c$ NAIVE
	$6kT_c$ "MFL"

NONE OF THESE CHANGE WITH T AT $T \subset T_c$

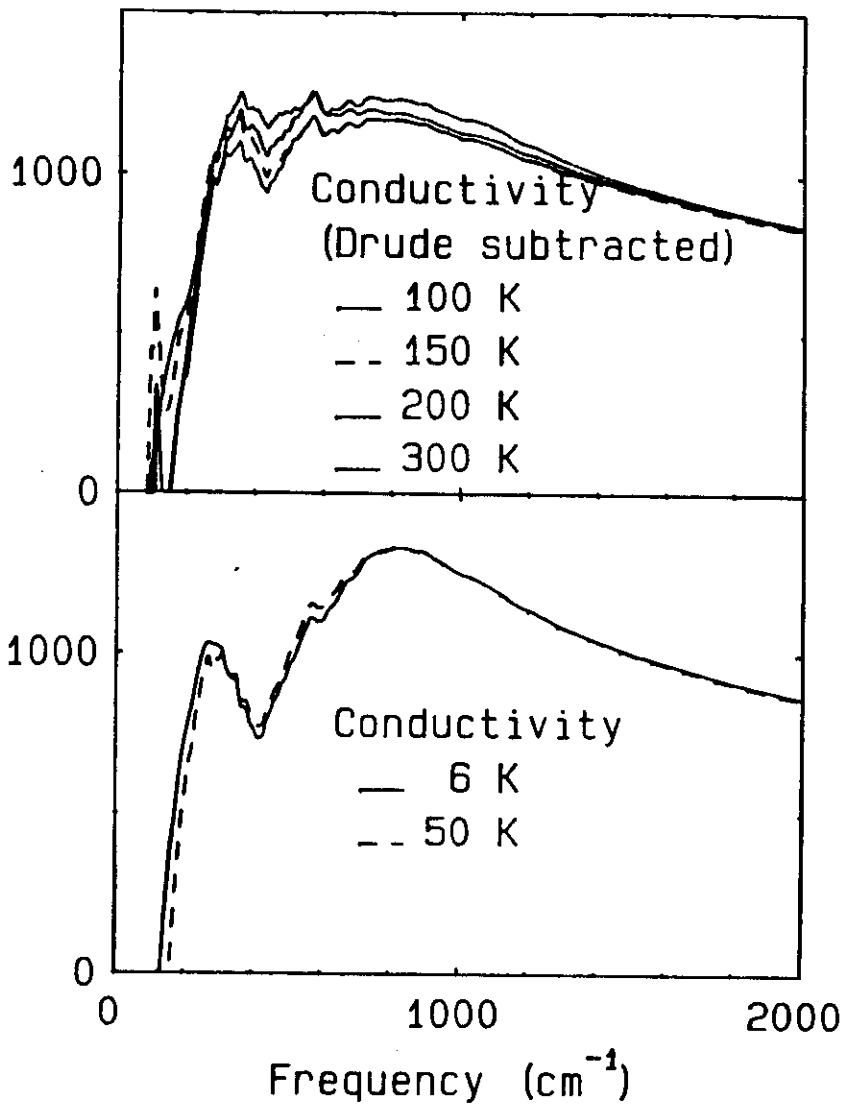

TWO-COMPONENT ABSORPTION + CLEAN LIMIT
($1/\tau < 2\Delta$)

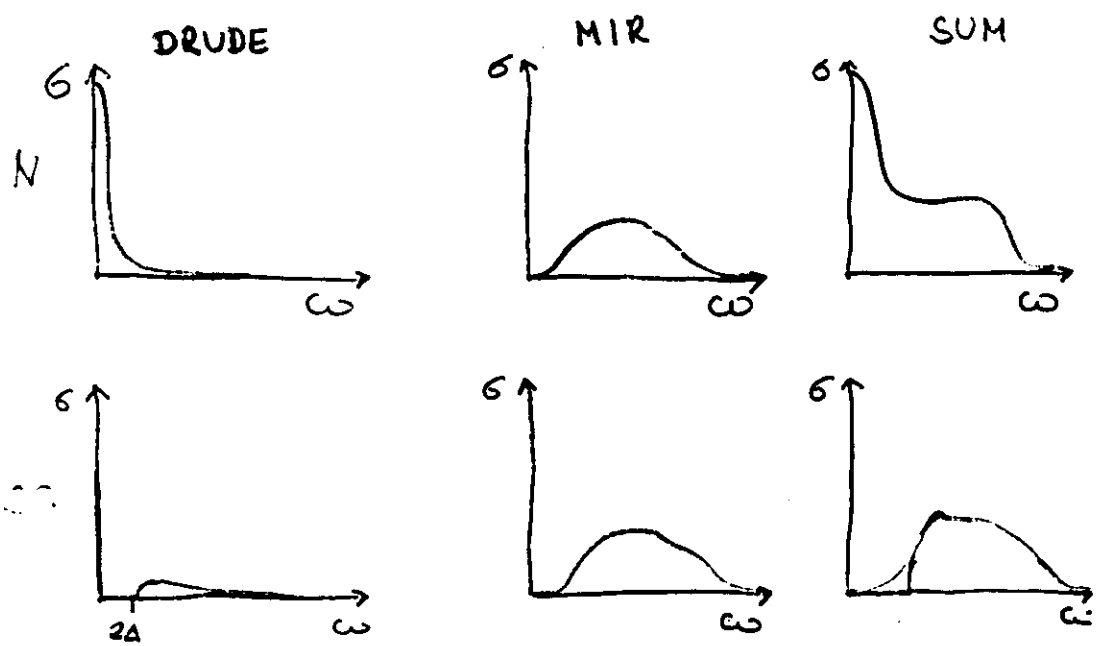

⇓

IMPOSSIBLE TO DETERMINE GAP
BY OPTICAL METHODS

DRUDE METAL:

$$\varepsilon(\omega) = \varepsilon_b - \frac{\omega_p^2}{\omega^2 + i\omega\Gamma}$$

if $\Gamma \to 0$

$$\varepsilon(\omega) = \varepsilon_b - \frac{\omega_p^2}{\omega^2} = \varepsilon_1(\omega)$$

THUS, FROM ε_1 vs. $\frac{1}{\omega^2}$ WE GET ω_p, ε_b

if $\omega \ll \Gamma$

$$\varepsilon_1(\omega) = \varepsilon_b - \frac{\omega_p^2}{\omega^2 + \Gamma^2} \cong \varepsilon_b - \frac{\omega_p^2}{\Gamma^2}$$

FROM $\varepsilon_1(\omega \to 0)$ WE GET Γ

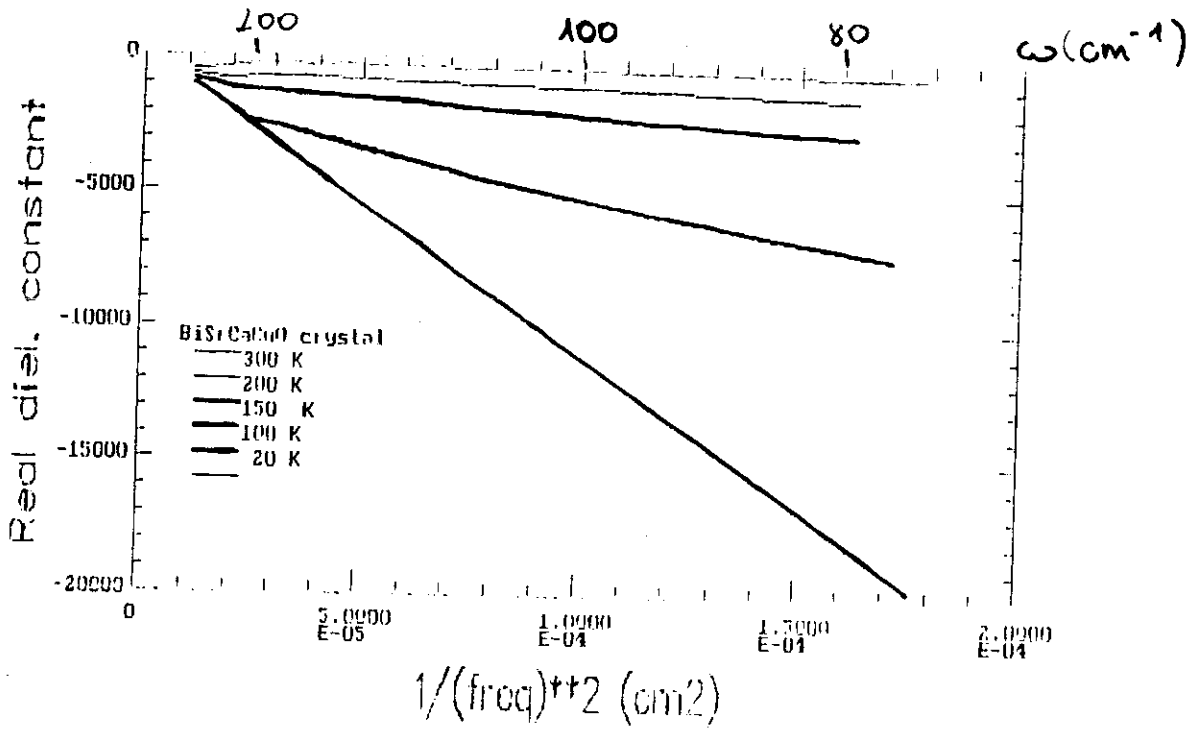
200
100
80
ω(cm⁻¹)
Real diel. constant
0
-5000
-10000
-15000
-20000
BiSrCaCuO crystal
300 K
200 K
150 K
100 K
20 K
0
5.0000 E-05
1.0000 E-04
1.5000 E-04
2.0000 E-04
1/(freq)**2 (cm2)

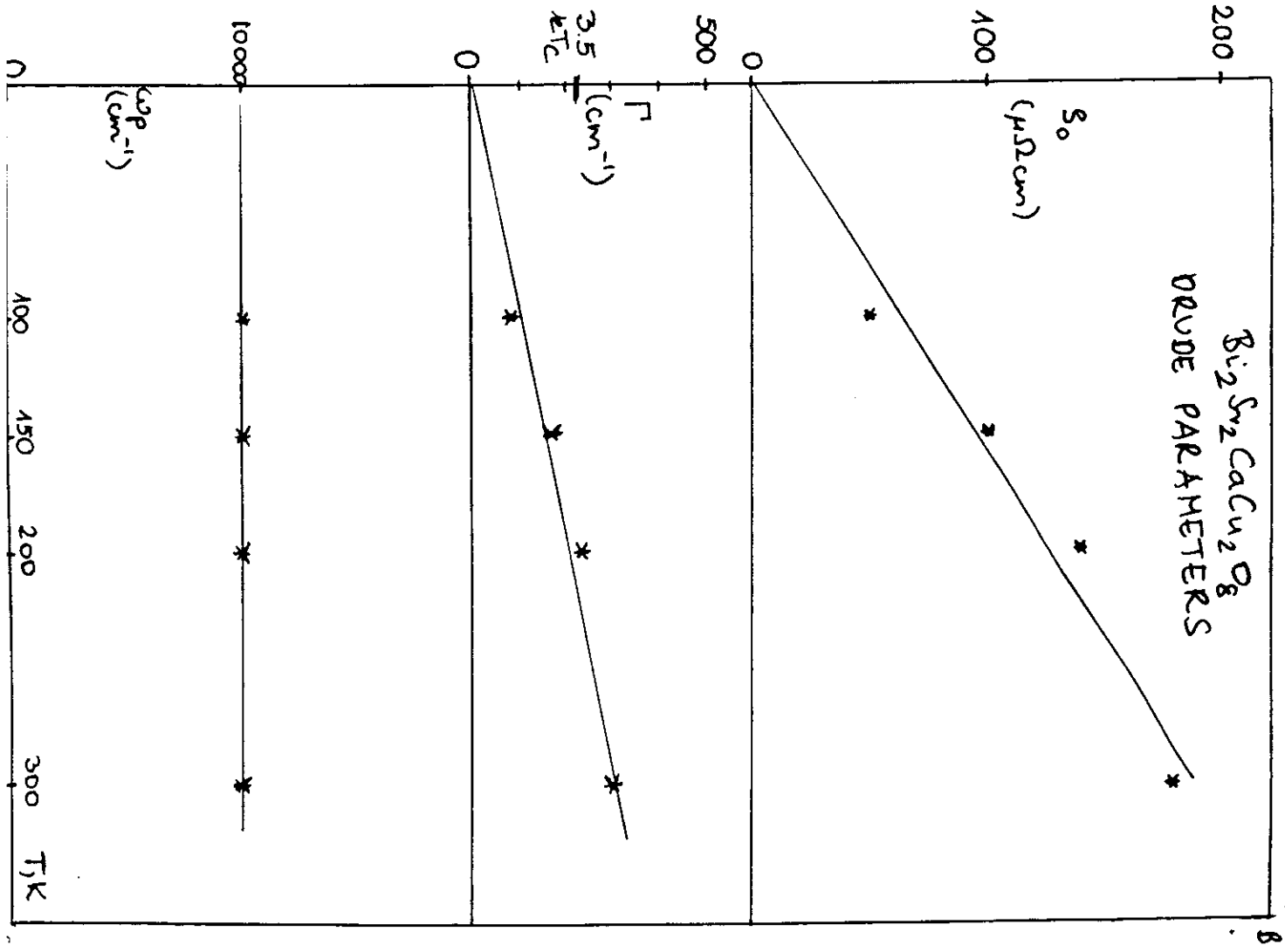
Bi2Sr2CaCu2O8
DRUDE PARAMETERS
S0 (μΩcm)
200
100
0
Γ (cm⁻¹)
500
0
3.5 kTc
ωp (cm⁻¹)
10000
0
100
150
200
300
T,K

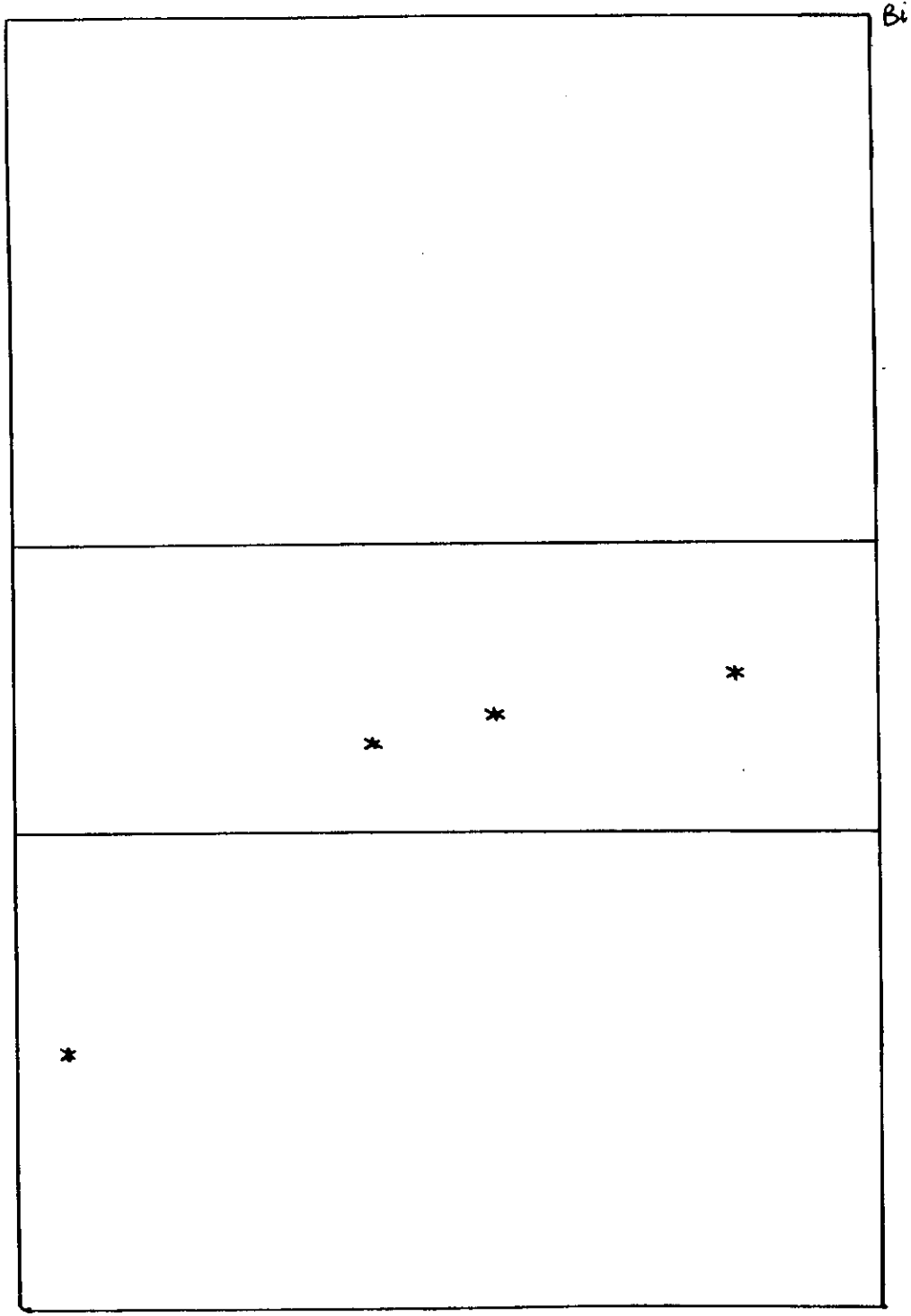

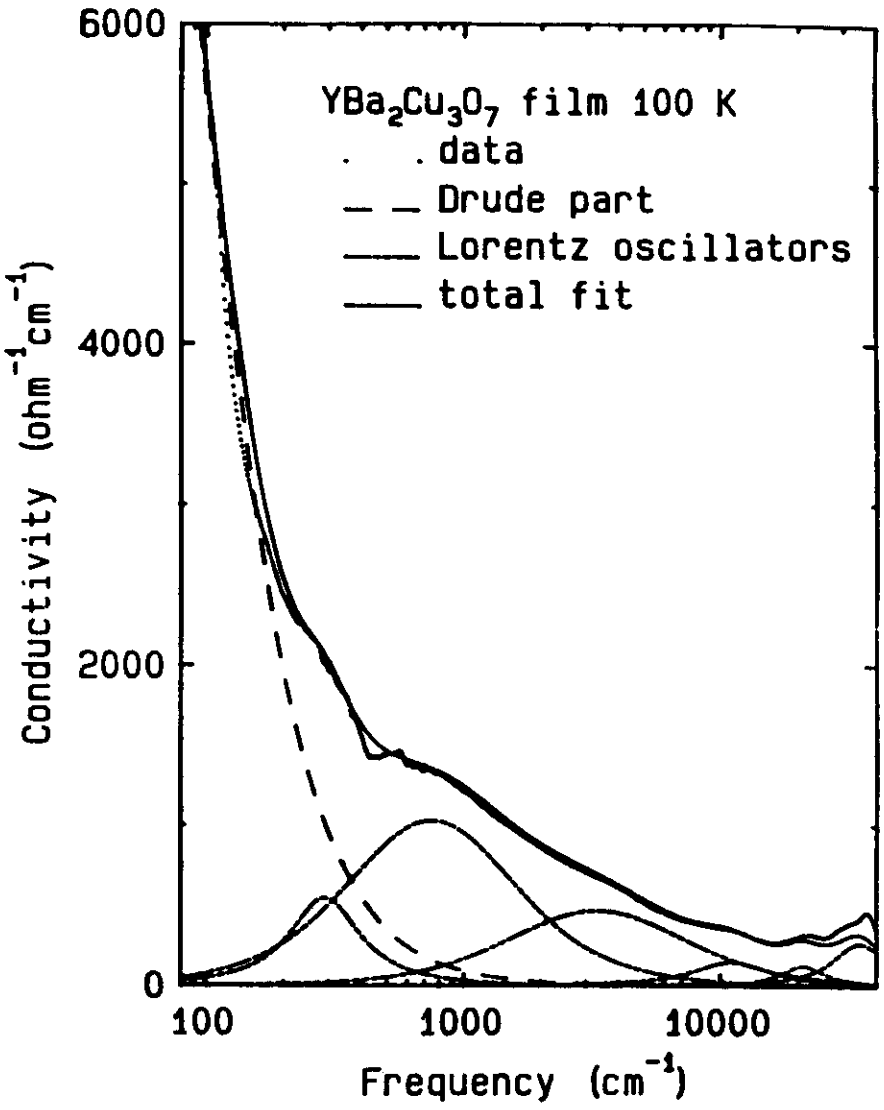
6000
4000
2000
0
100
1000
10000
Conductivity (ohm^{-1}cm^{-1})
Frequency (cm^{-1})
$YBa_2Cu_3O_7$ film 100 K
data
Drude part
Lorentz oscillators
total fit

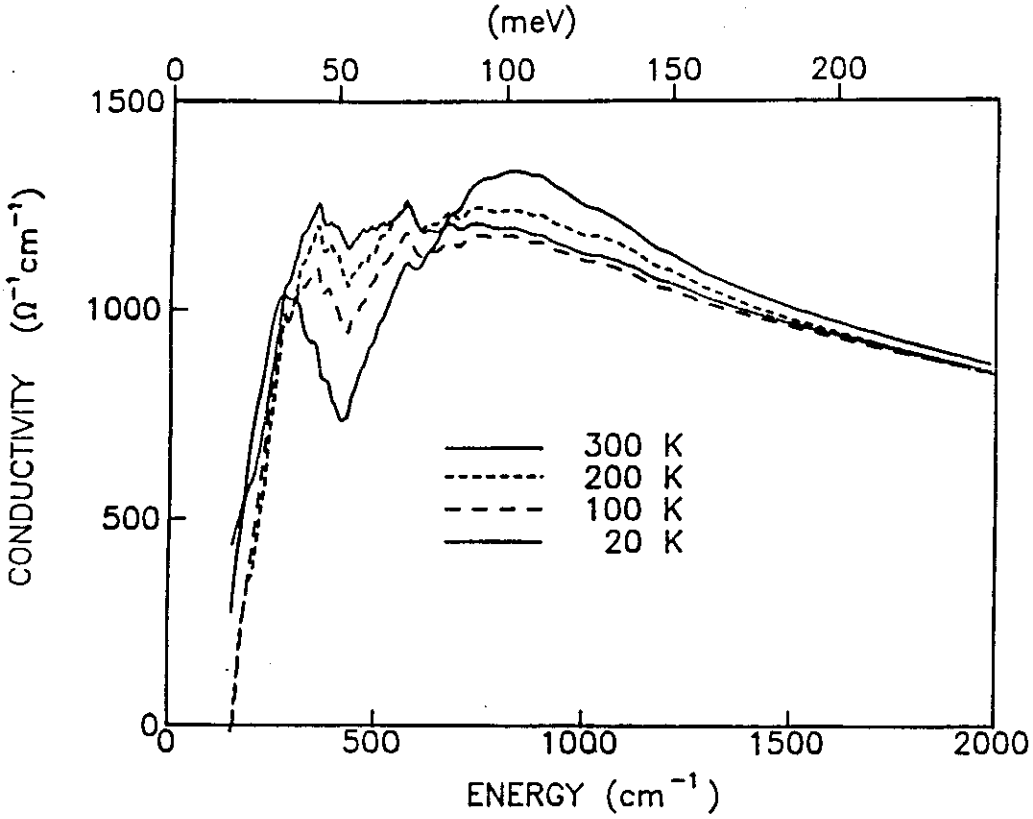
(meV)
0
50
100
150
200
1500
1000
500
0
CONDUCTIVITY ($\Omega^{-1}cm^{-1}$)
300 K
200 K
100 K
20 K
0
500
1000
1500
2000
ENERGY (cm^{-1})

Fig 1.

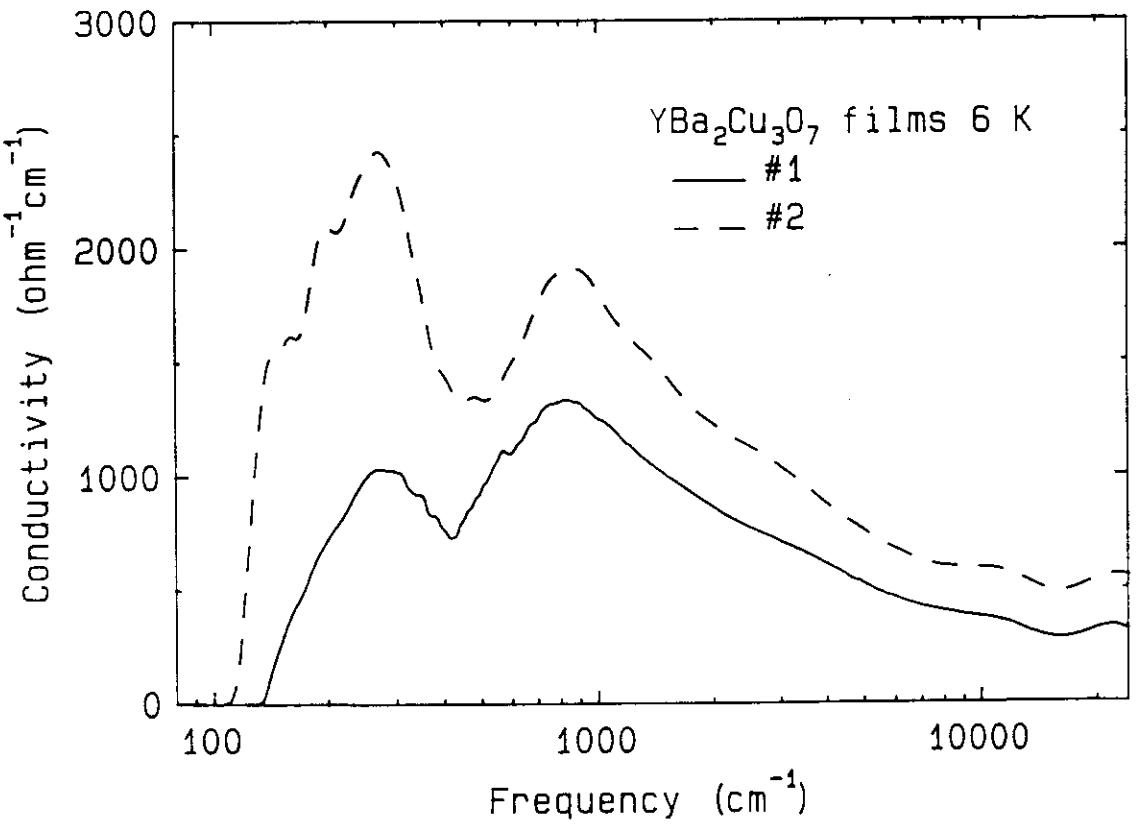
3000
2000
1000
0
Conductivity (ohm^{-1}cm^{-1})
$YBa_2Cu_3O_7$ films 6 K
#1
#2
100
1000
10000
Frequency (cm^{-1})

E-PH COUPLING TO 52 meV BRANCH:

$$\varepsilon(\omega) = \varepsilon_\infty + \varepsilon_D + \frac{\omega_{pe}^2}{\omega_e^2 - \frac{g^2}{m^* M \omega_0^2} D(\omega) - \omega^2 - i\omega\gamma_e}$$

$$D(\omega) = \frac{\omega_0^2}{\omega_0^2 - \omega^2 - i\omega\gamma_0}$$

$\left.\begin{matrix}\omega_{pe}\\ \omega_e\\ \gamma_e\end{matrix}\right\}$ ELECTRONIC BAND

$\left.\begin{matrix}\omega_0\\ \gamma_0\end{matrix}\right\}$ PHONON

$$\omega_g^2 = \frac{g}{\sqrt{m^* M}}$$ COUPLING FREQUENCY

T. TIHUSK & D. B. TANNER, 1989

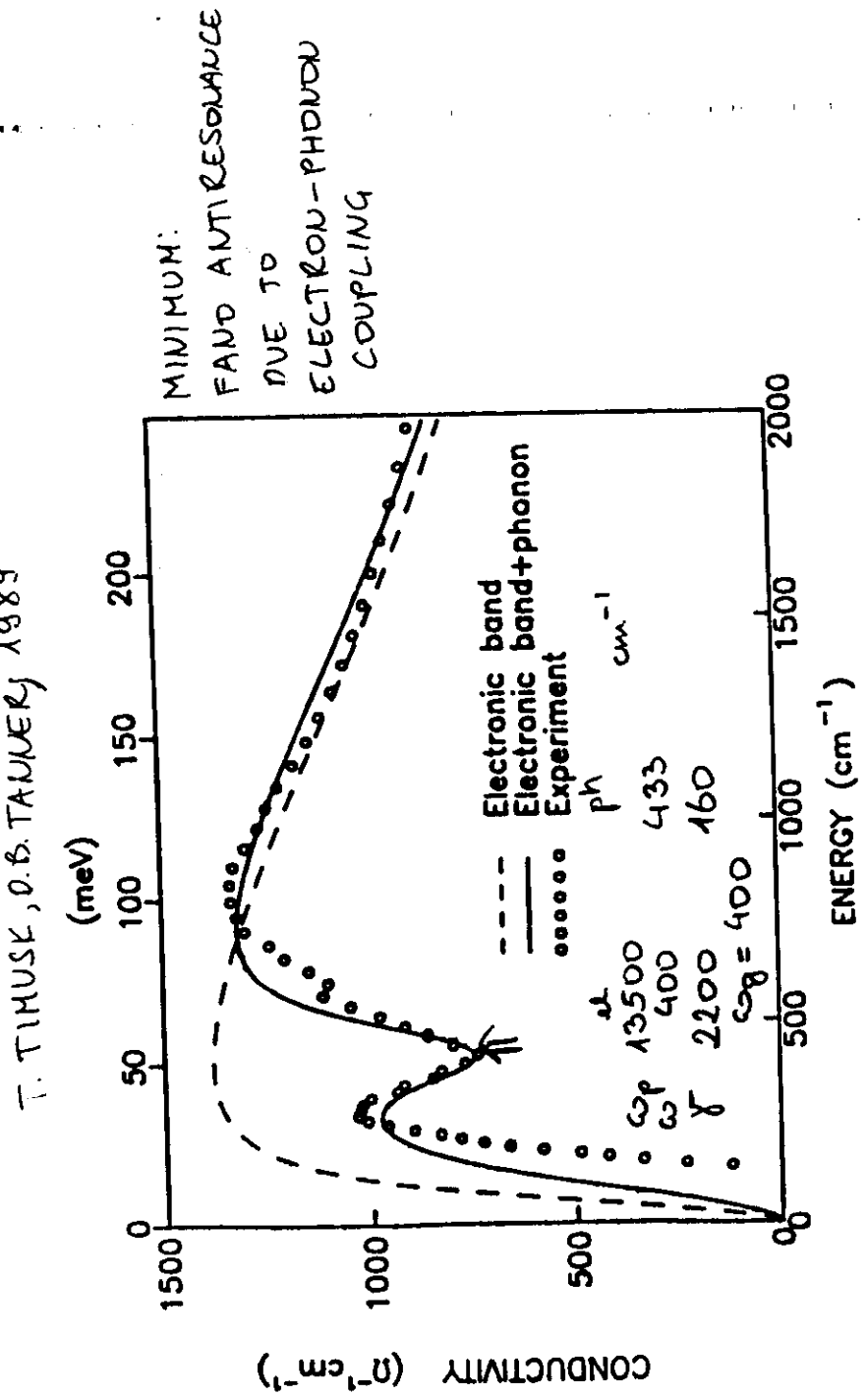

Fig 2.

CONCLUSIONS

ELECTRONS:

- NORMAL STATE:
  TWO-COMPONENT ABSORPTION

  1. NARROW DRUDE PART
  2. STRONG MID-IR BAND

- SC STATE:

  - CLEAN LIMIT
  - MID-IR BAND ONLY

PHONONS:

- NO SIGN OF DIRECT COUPLING ASSOCIATED WITH SUPERCONDUCTIVITY

- POSSIBLE COUPLING TO BOUND ELECTRONS

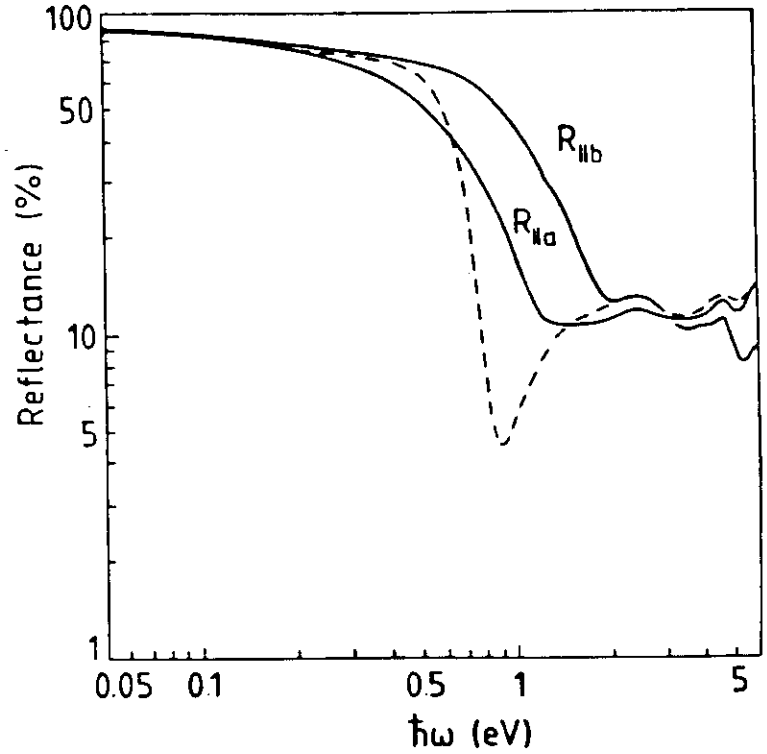

B. KOCH, H.P. GESERICH AND TH. WOLF:
SOLID STATE COMM. 71, 495 (1989)

Fig. 1

Z. SCHLESINGER ET AL:

Untwinned $Y_1Ba_2Cu_3O_7$ PRL 65, 801 (1990)

- a-axis
- b-axis

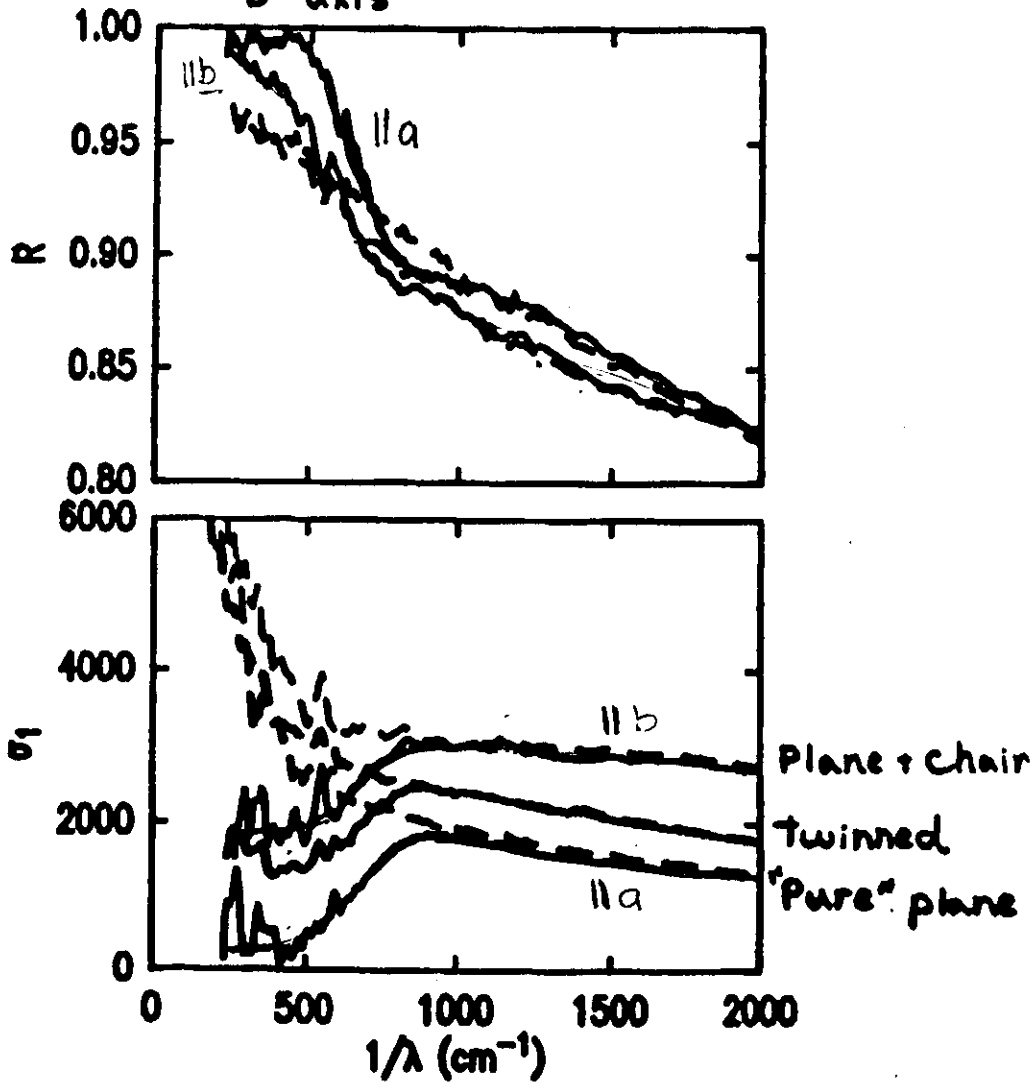

- $8 KT_c$ gap - planes - isotropic

D.B. ROMERO ET AL (1990)

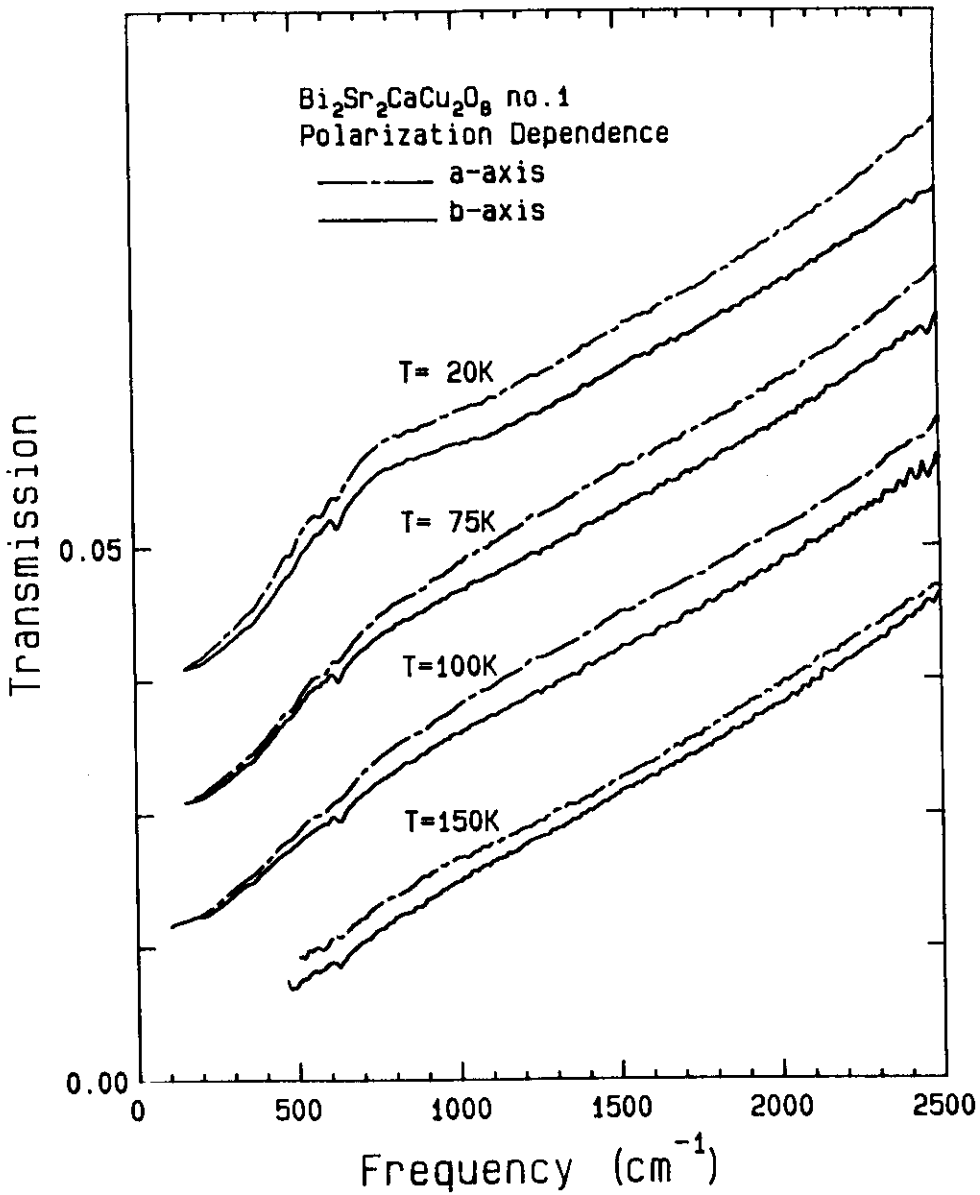

sufficiently close to the structural instability that even a single carrier locally changes the structure to that characteristic of the metallic (and superconducting) phase.

EXPERIMENTAL TECHNIQUES

The tetragonal semiconducting $YBa_2Cu_3O_{7-\delta}$ ($\delta \approx 0.75$) samples were prepared by heating orthorhombic superconducting material ($T_c = 92$ K: $a = 3.8170$ Å, $b = 3.8868$ Å, $c = 11.6721$ Å, $V = 173.26$ Å^3) in air at 850 °C in an alumina boat for 3 h followed by rapid quenching to room temperature. The resulting sample was not a superconductor; resistivity measurements gave the high dc value and characteristic temperature dependence of $\delta \approx 0.75$. X-ray powder patterns indicated a tetragonal unit cell: $a = 3.8590$ Å, $b = 3.8590$ Å, $c = 11.7949$ Å, $V = 175.65$ Å^3. The oxygen content was determined by comparing these values with the lattice constants given by Tarascon *et al.*[11] For photoinduced absorption, the sintered pellet was then reground to micrometer-sized crystallites and mixed at a concentration of 2 wt.% with KBr powder (for the spectral range from 400–4000 cm^{-1}) or 1 wt.% with CsI powder (120–500 cm^{-1}). The mixture was pressed into thin dark grey semitransparent pellets, which were then reground and repressed to achieve greater homogeneity. This process was repeated until satisfactory transparency and homogeneity was achieved.

An IBM/98 (Bruker) Fourier-transform ir interferometer, modified to allow access onto the sample of the external beam from an Ar^+ laser, was used to cover the spectral range from 120 (0.015 eV) to 4000 cm^{-1} (1 eV); the CsI cutoff set the low-frequency limit. For temperature control, the sample was placed on the cold finger of an Air Products Heli-tran system. The sample was optically pumped by the laser at 2.7 eV with a power level of 30 mW/cm^2, and the fractional changes in ir transmission were measured[13] (with resolution of 2 cm^{-1} in the far-infrared region and 4 cm^{-1} in the mid-infrared region). The net change in the absorption coefficient ($\delta\alpha$) was determined from the photoinduced change in transmission (ΔT); for small ΔT, $-\Delta T/T = \delta(\alpha d)$ where d is the sample thickness. To obtain an acceptable signal-to-noise ratio, signal averaging (~2 h) was required.

EXPERIMENTAL RESULTS

Figure 1 shows the photoinduced absorption spectra for the semiconducting tetragonal phase $YBa_2Cu_3O_{7-\delta}$ ($\delta \approx 0.75$) obtained in the spectral range from 120 to 4000 cm^{-1} at 15 K, with the inset showing the photoinduced IRAV modes in greater detail. We found three major IRAV modes at 396, 436, and 520 cm^{-1} and four major photoinduced bleachings at 192, 219, 362, and 598 cm^{-1}. In addition, a broad electronic absorption peak at 1050 cm^{-1} (~0.13 eV) was observed.

In Fig. 2 we compare the ir spectra of $YBa_2Cu_3O_{7-\delta}$ ($\delta \approx 0.75$) at 15 and 300 K, with the ir spectrum of superconducting $YBa_2Cu_3O_{7-\delta}$ ($\delta < 0.2$). For $\delta \approx 0.75$, vibrational modes were found at 164, 191, 216, 252, 361, 472,

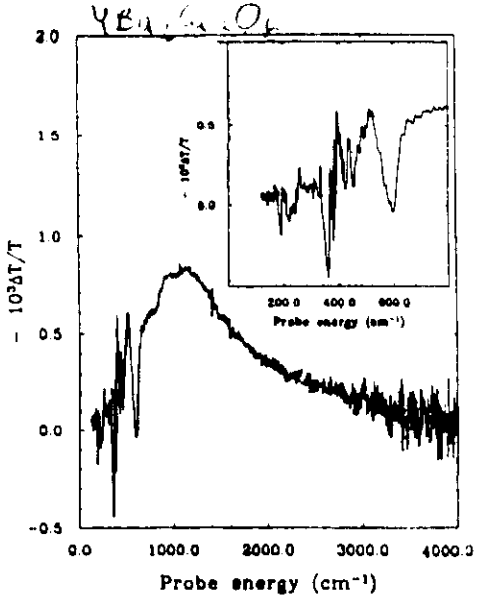

FIG. 1. Photoinduced absorption spectrum of $YBa_2Cu_3O_{7-\delta}$ ($\delta \approx 0.75$) at 15 K (2.7-eV pump at 30 mW/cm^2); inset shows detailed IRAV features.

KIM ET AL.: PRB 38, 6478 (1988)

532, 583, and 632 cm^{-1} with the sample at 300 K. Upon cooling to 15 K, we observed an increase in oscillator strength of the 359-cm^{-1} mode and a 10-cm^{-1} blueshift of the 583-cm^{-1} mode, consistent with values reported earlier.[12] For the orthorhombic phase ($\delta < 0.2$), we observed relatively weak ir vibrational features at 336, 454, 493, 528, and 602 cm^{-1} at 300 K. They appear weak in transmission due to the strong free-carrier background in the highly conducting sample. Reflectivity data[14] show quantitatively that the 528- and 602-cm^{-1} absorptions are relatively weak compared to the modes below 400 cm^{-1}. In contrast, for the tetragonal phase we find that the modes at 532, 586, and 632 cm^{-1} are much stronger than those in the far-infrared region. The ir modes associated with the two structures can be compared with the photoinduced features shown in Fig. 1 (IRAV modes at 396, 436, and 520 cm^{-1} and bleachings at 192, 219, 362, and 598 cm^{-1}). In particular, the bleaching frequencies suggest that photoexcitation locally converts the structure from tetragonal to orthorhombic.

Artifacts associated with the photoinduced absorption technique can be generated by sample heating by the incident laser pump beam. In systems such as oxide superconductors, small changes in the "dark" ir absorption caused by a strong temperature dependence can be incorrectly interpreted as photoinduced absorptions. Small shifts in frequency with changes in temperature would appear as derivative-shaped signals in the photoinduced spectra; changes in linewidth would appear as second-derivative-shaped signals. Similarly, a decrease in intensity